Sci. Annals. Fac. Phys. & Mathem., Univ. Thessaloniki, 20b, 83 (1980)

# INFRARED AND RAMAN STUDIES OF THE VIBRATIONAL PROPERTIES OF AMORPHOUS SEMICONDUCTORS

By

D. I. SIAPKAS

*2nd Laboratory of Physics*
*Physics Dept., University of Thcssaloniki, Greece.*

**Abstract:** *Nowdays Raman and Infrared spectroscopy are well developed tools for studies of atomie vibrations, chemical bonding and local atomic arrangement in a sense complementary to X-ray, Elcctron and Neutron diffraction probes. This paper gives a physieal picture of the amorphous state, the breakdown of crystal selection rules and the appearanec of disorder induced IR and Raman vibrational spectra. Morcover the physical prineiples involved in the reception, analysis and interpretation of IR and Raman spectra are prescnted. Applications of these methods are illustrated for prototype tetrahedral Ge, Si, GaAs and chalcogenide S, Se, $As_2S_3$, $GeSe_2$ elemental and compound amorphous semiconductors as well as for the binary alloys $As_{1-x}Sc_x$, Si-H. In addition the vibrational properties of the ferroelectric semiconduetive SbSBr compound and $[AsSI]_{1-x}$ - $[SbSI]_x$ solid solution, at the transition from crystalline to amorphous phase, are discussed.*

## 1. INTRODUCTION

Due to intensive research and new revolutionary technologies glasses and other non-crystalline solids are becoming materials of tremendous technological importance like the other groups of machinable materials, metals, polymers and ceramics. One-two decades ago the world knew mainly bottles, lenses, crystal and window glass; nowdays highly sophisticated materials as glassy waveguides, bioglasses, glassy metals, semiconducting glasses and various types of glass-ceramics are in great demand. But unlike crystalline solids, amorphous are materials difficult to understand and correlate fundamental properties and structure. Structure determinations of amorphous materials have steadily progressed since the first application of X-ray and electron diffraction and Infrared and Raman spectroscopy methods to the study of liquids and glasses. However, in spite the successive improvements in experimental

methods and the increasingly refined models have widened our knowledge of the short-range order (SRO) in amorphous materials even the choice between "continuous network" [1] or "crystallite" [2-3] hypotheses can not be made and still is debated.

Raman and IR spectroscopy are well developed tools for the study of atomic vibration and the composition of the structural (chemical) units forming binary, ternary and even more complex amorphous materials. They are in a sense complementary probes to X-ray and electron diffraction. In general, diffraction studies of the radial density function has been the major source of experimental information on the structure of elemental semiconductors, while vibrational spectroscopy has been most valuable in studies of compound or alloys whose vibrational response can be traced to that of a basic "molecular" unit. The determination of local order in amorphous semiconductors by IR and Raman spectroscopy must be considered as indirect when compared with the standard diffraction techniques. It is not possible to process the measured spectra with well established algorithms and thus obtain the desired information about Short Range Order. Ruther, one postulates a certain model for this order and calculates the shape of the spectra to be observed. Comparison with the experimental spectra enables one to decide which model is more likely to correspond to physical reality. Another useful method consists of comparing the observed spectra with the spectra of other materials which contain similar radicals in a well-known S.R.O. configuration. While these methods have the advantage of also providing information about the vibrational structure of a given material in relation to its S.R.O., the information obtained about the order itself is at best only of semiquantitative nature. It is also subject to errors. Different configurations, one of which may not have been considered in the analysis, could have similar vibrational properties.

It is the purpose of the present paper to give a physical picture of the amorphous state of the "3-dimension network" and "molecular" type solids and the physical principles involved in the reception, analysis and interpretation of IR and Raman spectra. The methods will be illustrated for:

I. Prototype elemental Ge, Si and compound GaAs tetrahedrally coordinated amorphous semiconductors (films).

II. Prototype elemental chalogens S, Se and chalcogenide compounds $As_2S_3$, $GeS_2$ (Glasses).

III. Binary alloys $As_{1-x}X_x$, $Ge_{1-x}X_x$ (X = S, Se) and Ge-H, Si-H. These alloys are currently of great interest for their application in xerographic photoreceptors the first group and in electronic and photoelectronic junction devices the last.

IV. Glasses of the ferroelectric semiconductive $A^{V}B^{VI}C^{VII}$ compounds, SbSBr, AsSI, AsSI-SbSI, which we are studying for long time at our laboratory. These are the most probably ferroelectric glasses, they have high diffraction index, low glass transition temperature Tg and their significance for IR devices çan be realized from Fig. 21.

The experimental procedures, theory and IR, Raman and Neutron spectra for various glass systems are summarized in a number of review articles [4-9]. Very good sources of information are the proceedings of the last Int. confer. on Amorphons and Liquid Semiconductors [10] and also the Proceedings of the last two biannual International Conferences on the Physics of Semiconductors [11, 12]. The growth in the number of contributed papers on the subject of disordered or amorphous semiconductors was such that seven sessions had to be organized, including laser annealing, at the Kyoto Conference in 1980 [12].

## 2. STRUCTURAL DISORDER - THE AMORPHOUS STATE.

The amorphous state is characterized by what it is not [13]. It is not a form of matter with long range order (LRO), it does not have large regions in which the atoms are arranged in a periodic way, there are no crystallites of a size large enongh to give sharp Bragg X-ray and electron diffraction rings or spots [4]. While a review of the amorphous state is beyond our scope here, it is important to give the reaader two warnings.

### *2.1 The symmetry of amorphous*

First the term "disordered" is more general than "amorphous" and can refer to crystals as well as glasses. Substitutional disordered systems (Fig. 1a) are crystals (mixed or solid solutions) in which the disorder arises from impurity atoms snbstituted for a host atom. Usually the crystal can be treated as if the atom positions still maintain a regu-

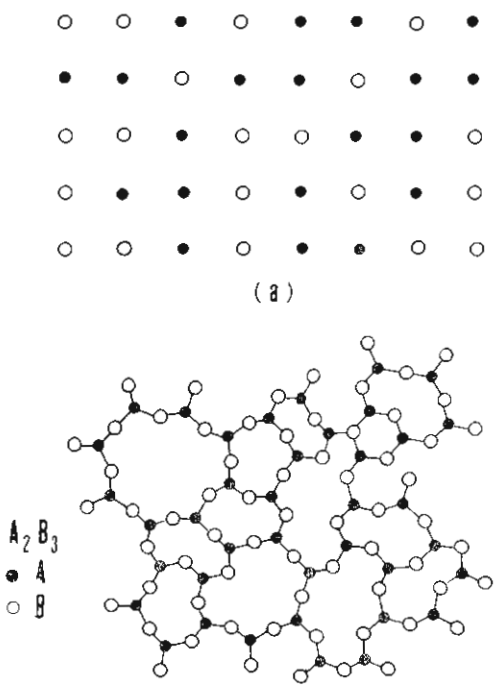


*Fig. 1. Schematic representations in two dimensions of disordered systems (a) substitutional disorder (mixed crystal) (b) Structural disorder, random network. Trigonal SRO is retained in the $AB_{3/2}$groups.[15].*

lar periodic array and the principal perturbation is only one of a mass change. Experimentally, such crystals show fairly sharp X-ray and electron diffaction lines. In the structural disorder material or amorphous (Fig. 1b) the disorder affects the periodic arrangement itself. In Fig. 1b is shown the widely quoted representation of amorphous state proposed by Zachariasen [1]. The figure schematically depicts a two-dimensional $A_2B_3$ structural disordered solid, with no LRO. Differing bond lengths and bond angles can cause a loss of both SRO and LRO which would have been present in crystalline $A_2B_3$. In the two -dimensional network representation of Fig. 1b one can identify always an $AB_3$ triangle unit as a "molecular" unit but it depends on the relative softness of the bond bending force constants associated with the B atoms, which bridge together the supposed strongly bonded $AB_3$ groups, if the solid can be considered as a suitable candidate for "molecular"

type analysis. The Zachariasen picture has been criticized since its inception, but not single model has taken its place. The key to the definition of the "amorphous" is the distinction between long and short range ordering. In practice, simple amorphous materials have strong short range ordering for distances out to three or four bond lengths. Longer range correlations are not observed except in crystals. There appears to be a lower limit on crystallite size (30-40 Å for Si) and an upper limit on the correlation length in amorphous semiconductors (12-15 Å for Si).

### *2.2 The glass transition and $T_g$ temperature*

In this article and the literature some authors use the terms amorphous, non-crystalline, glassy and vitreous synonymously. Others define a glass as an amorphous solid which can be prepared by supercooling a melt. By its very nature ordinary melt-quenched glass is thermodynamically unstable and can transform with time or on heating, first towards a metastable (supercooled melt) above the glass tran-

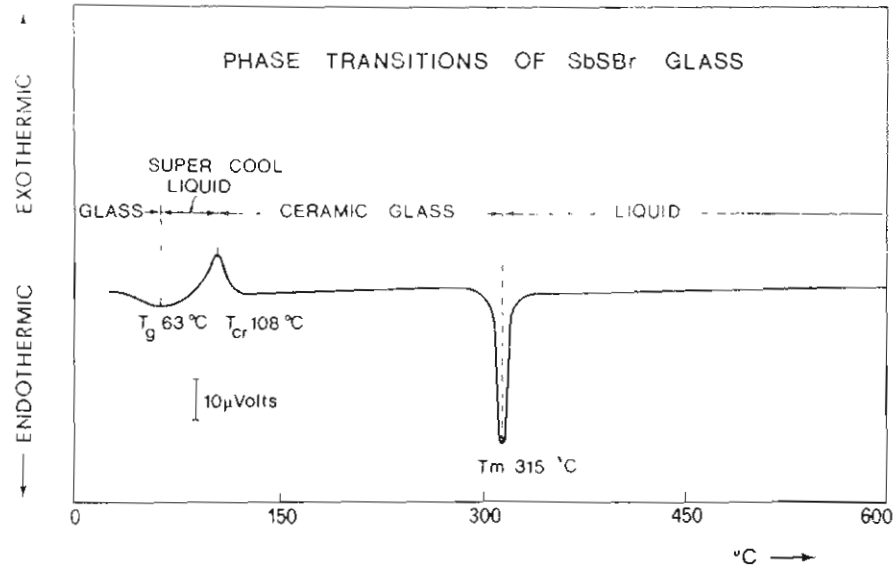


*Fig. 2. Differential Thermal Analysis (D.T.A.) thermograms of the unstable SbSBr glass, showing the successive phases; metastable supercooled melt above the glass transition Tg, stable ceramic glass above the erystallization temperature $T_{cr}$ and melt above the melting point $T_m$. [Unpublished data].*

sition temperature Tg and then to a stable phase (crystalline or glass-ceramic) above the crystallization temperature Tcr (Fig. 2). Different preparation techniques from solid, liquid or vapour phases by fast processes, which essentially cause an excess of free energy to be more or less temporarily "frozen in" to the material, may yield different amorphous forms of the material. Amorphous $As_2S_3$ [14]e.g. may be precipitated from a solution of $As_2O_3$ in a dilute hydrochloric acid solution by passing $H_2S$ gas and similarly, amorphous $Sb_2S_3$ from an acid solution of $SbCl_3$. In both cases the amorphous precipitates show (Fig., 3) typical glass transition behavior on heating with Tgs very close to those observed for a melt-quenched $As_2S_3$ sample ($Tg \simeq 480^0K$) and a sublimed $Sb_2S_3$ sample ($Tg \simeq 495^0K$). It also appears from spectroscopic studies that the major spectral peaks are insensitive to the details of sample preparation in many cases.

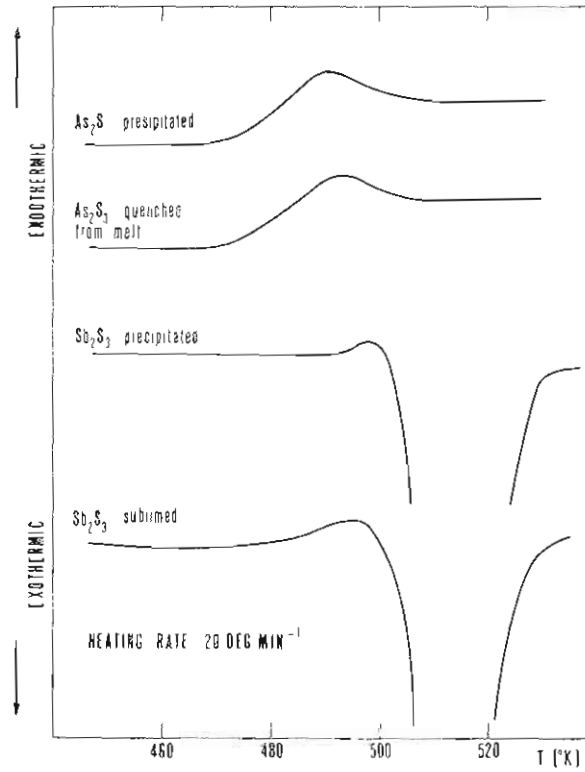


*Fig. 3. Differential Scanning Calorimetry (D.S.C.) thermograms for chemically precipitated and quenched from the melt $As_2S_3$ and preeipitated and sublimed $Sb_2S_3$.[14].*

## 3. DISORDER INDUCED IR AND RAMAN VIBRATIONAL SPECTRA

In crystals, the long-range order allows one-phonon absorption or scattering processes only for K-vector close to $K = 0$. Disorder makes it possible to couple light to K-vectors far from the origin and the spectra probe in an indirect way, through the density distribution function $g(\omega)$, the phonon dispersion relations [7], [16-18].

Infrared spectroscopy is associated with an absorption process. The absorption depends on the formalism of an electric dipole of moment $\vec{M}$ by the vibration. In a crystalline solid, the tesultant $|\vec{M}.\vec{E}|$ can be non-zero only if the K-vector of the incident electromagnetic radiation $\vec{K}_i$ is equal to the K-vector of the vibration $\vec{q}$. From energy conservation it follows that the frequency $\omega_i$ of the absorbed radiation is equal to the frequency $\Omega$ of vibration. So for the crystals the conservation rules for infrared absorption are

$$\omega_i = \Omega \tag{1}$$

$$\vec{K}_i = \vec{q} \tag{2}$$

The frequency $\Omega$ of the phonon (quantum of vibration energy) varies with momentum throughout the Brillouin zone edge determined by a wave vector $q_{max} = 2\pi/\alpha \sim 10^8$ cm$^{-1}$ for typical values of the crystal lattice constant $\alpha$. As $K_i = 2\pi/\lambda_i \sim 10^5$ cm$^{-1}$, for a visible photon, is very small compared to $q_{max}$, the radiation practically couples to $q \simeq 0$

Raman, or inelastic scattering of light, is produced by the modulation of the electrical polarizability by vibration. As for all scattering processes we have conservation of the K-vector and energy

$$\omega_s = \omega_i + \Omega \tag{3}$$

$$\vec{K}_s = \vec{K}_i \pm \vec{q} \tag{4}$$

where the + sign refers to anti-stokes, — sign to stokes lines, and $\omega_s$, $K_s$ refers to scattered Raman light. From eq. (4) it follows again that in a crystal we couple practically to phonons with $q = 0$.

In addition to eqs. (1)-(4) there are other selection rules for IR and Raman activity that pertain to the symmetry of the vibrational modes. The basic differences between the IR and Raman spectra are associated with the difference of the symmetry which is described by a vector (dipole moment) for the absorption process and by a symme-

trical tensor (Raman tensor) for the scattering. The difference is most pronounced if the crystal (or the molecule) has a center of symmetry. Then the vibrations can be classified as either even or odd. The dipole transitions are forbidden for even symmetry, the scattering for odd symmetry. Therefore the IR spectra show the odd vibrations, the Raman spectra the even vibrations, and both spectra ave complementary. If there is no center of symmetry, the selection rules are more complicated. But still the most intensive lines of the IR spectrum are weak in the Raman spectrum, and vice-versa.

The other conseqnence of the different symmetry of both effects is the different averaging in disordered systems. The IR absorption of a powdered anisotropic crystal or of molecules in a gas, does not depend on light polarization. The Raman spectra are sensitive to the local assymmetry in the scattering material and we can obtain some information [19] by measuring the depolarization ratio of the scattered light

$$\rho = I_{VV}/I_{VH} \tag{5}$$

with the polarizations of the incident and scattered beams in parallel ($I_{VV}$) or at right angles ($I_{VH}$).

The conservation (or selection) rules expressed by eqs. (2) and (4), involve crystal momenta and therefore in the amorphous solid are relaxed or brokendown. In some systems all the energy-allowed vibrational modes can become optically active, at least as far as the momentum selection rules are concerned. If the short-range order is the same in the amorphous and crystalline case, one can try to use the phonon dispersion curves Fig. 12, of the crystal, and assume that phonons with the K-vector in the whole first BZ contribute. If we further assume that the K-dependent weighting factors and the matrix elements are approximately constant than the IR and Raman spectra should be continuoua in the first approximation similar to the one-phonon density of states $g(\omega)$ which may be a broadened version of $g_c(\omega)$ in the crystal (Fig. 12). In addition, there should be a similarity between the IR and Raman spectra because the disorder tends to make ineffective the selection rules imposed by the crystal symmetry. Actually the IR and Raman spectra of amorphous semiconductors are modulated by matrix element dependent terms which reflect the symmetry of the local atomic environments. This dependence on an one-phonon density of states, $g(\omega)$ and matrix element effects can be included in generalized expressions for the ir-absorption, $\alpha(\omega)$ or the Raman scattering.

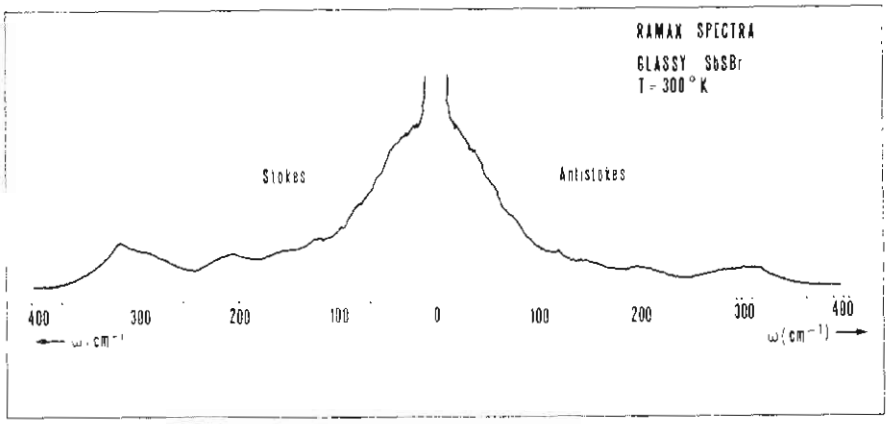


*Fig. 4. A direct trace of a typical room temperature. Stokes and Anti-Stokes Raman spectrum of SbSBr glass obtained at a 90° seattering geometry. [Unpublished data].*

## 4. REDUCED RAMAN AND INFRARED SPECTRA

The above crude reasoning explains the main qualitative features of the IR and Raman spectra of tetrahedrally bonded amorphous semiconductors elemental Si [20-22], Fig. 11, Ge [23,21.22], and compound GaAs [23,22]. For a meaningful comparison of the measured Raman spectra $I(\Omega)$ and infrared spectra to the density $g(\omega)$ of vibrational states, one must reduce the measured Raman spectra $I(\Omega)$ by a factor which is related to the population of the vibrational states by phonons. In 1970 Shuker and Gammon [16] presented a calculation for the Raman effect according to which the reduced intensity $I_R(\Omega)$ of stokes lines is

$$I_R(\Omega) = \Omega(\omega_i - \Omega)^{-4}[n(\Omega)+1]^{-1}I(\Omega) \qquad \text{Stokes} \qquad (6)$$

where

$$n(\Omega) = [\exp(h\Omega/kT)-1]^{-1}$$

is the Bose-Einstein distribution function at the temperature T. The anti-stokes component is similarly

$$I_R(\Omega) = \Omega(\omega_j + \Omega)^{-4}n(\Omega)^{-1}I(\Omega) \qquad \text{Antistokes} \qquad (7)$$

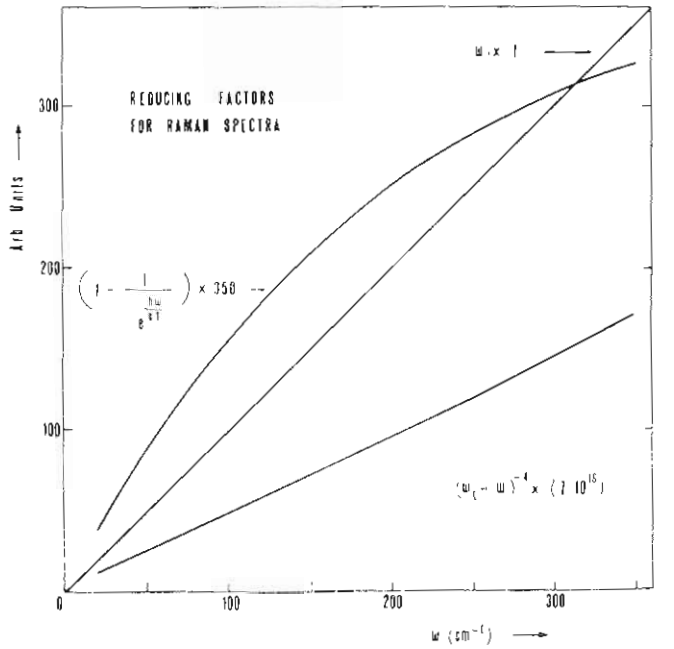


*Fig. 5. The relative contribution of the three reducing factors of eq. (6). Notice the scale.*

The reduced Raman $I_R$ ($\Omega$)involves matrix elements, (selection rules) but does not contain any temperature dependent statistical factors. For first-order IR absorption, there are no statistical correction factors. A temperature dependent $I_R(\Omega)$ or infrared absorption is indicative of higher order multiphonon or other type anharmonic processes. Here again, we note that $\omega_j$ is the frequency of the incident laser light, $\omega = \omega_j \pm \Omega$ is the frequency of the scattered light in the Stokes(-) and Antistokes (+) spectrum and $\Omega$ is the Raman shift. Experimentalists have found the SG result extremely useful for producing reduced Raman spectrum free of spurious structure due to thermal population effects, espessially in the very low frequency region 0-100 $cm^{-1}$. A picture of a direct trace on the recorder paper of a typical room temperature spectrum of SbSBr glass is shown in Fig. 4. The stokes and antistokes unpolarized spectrum, free of any plasma or ghost line, was obtained in a $90^0$ transmission scattering geometry with 70 mW of a 6471 Å Kr laser line on a Spex Ramalog 5 double monochromator. Since at room temperature most molecules are in the vibrational gro-

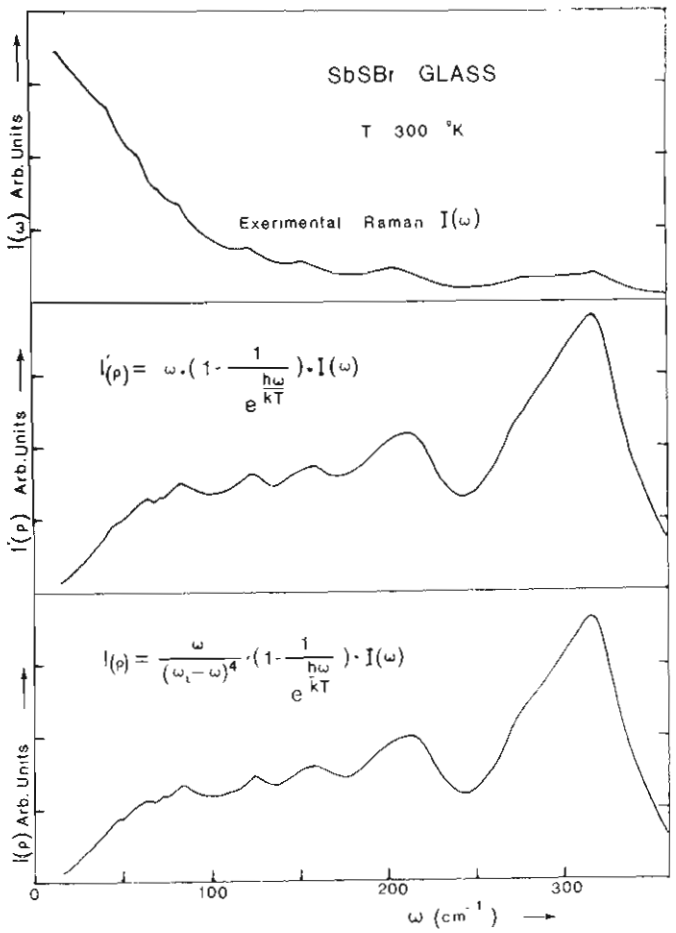


*Fig. 6. Experimental $I(\omega)$ and redueed $I(\varrho)$ Raman speetra of SbSBr glass. In the middle spectrum $I'(\varrho)$ the factor $(\omega_L-\omega)^4$ has not been used but $I'(\varrho)$ and $I(\varrho)$ are almost the same.*

und state, the antistokes lines, which originate from higher energy states, are typically much lower in intensity than the corresponding stokes lines. The experimental spectrum $I(\omega)$ has been reduced, in Fig. 6, with the factors of eq. (6) and eq. (7) whose relative contribution is plotted in Fig. 5. It is easily seen the very small contribution of the extra radiation factor of $(\omega_i \pm \Omega)^4$ [in the figures is written $(\omega_L-\omega)^4$] and in most cases can be neglected. In the reduced Raman spectrum of Fig. 6, free from the spurious low frequency (below~150 $cm^{-1}$) stru-

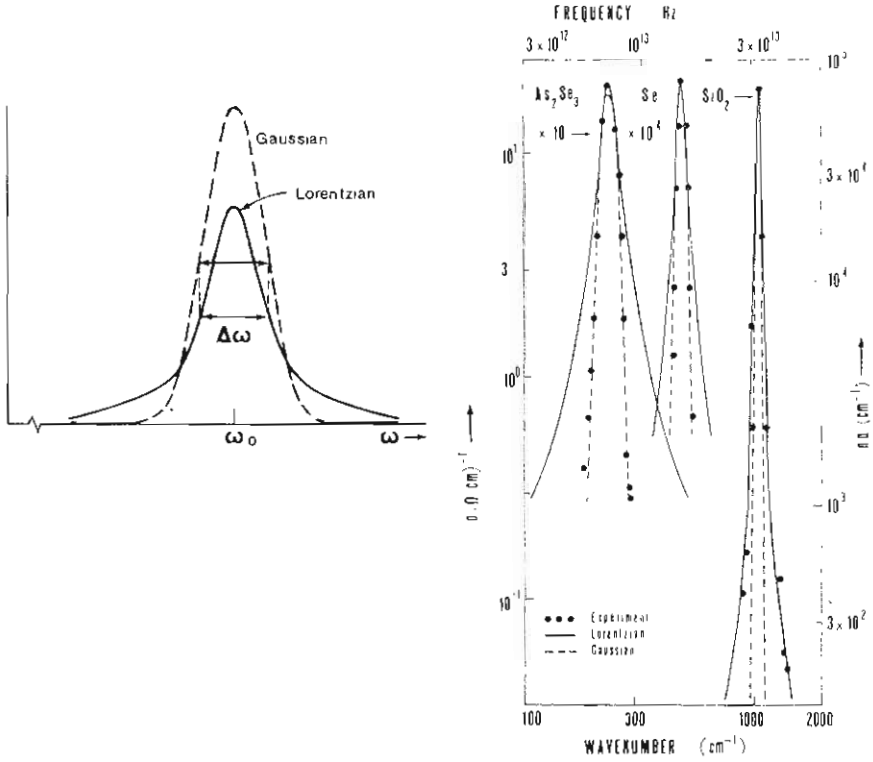


*Fig. 7. Comparison of Gaussian and Lorentzian line-shapes of same linewidth.*
*Fig. 8. Fitting of conduetivity spectra with Gaussian and Lorentzian oscillators for three representative glasses with predominently 1-D(Se), 2-D($As_2Se_3$) and 3-Dimension ($SiO_2$) networks. The line-shape of $SiO_2$ is Lorentzian.*

cture, all the nine bands can be seen.

In Shuker and Gammon calculations [16] they have considered

$$I_R(\Omega) \sim \sum_b C_b^p \, g_b(\omega) \tag{8}$$

the polarization-dependent coupling $C_b^p$ in various vibrational subbands b as constant. Recently Galeener and Sen [24] have proposed new expressions with which Raman and IR spectra of amorphous solids can be compared on an equivalent basis by contrasting the reduced Raman spectrum

$$I_R(\Omega) \sim \sum_b C_b^p \, (\omega) \, g_b(\omega) \tag{9}$$

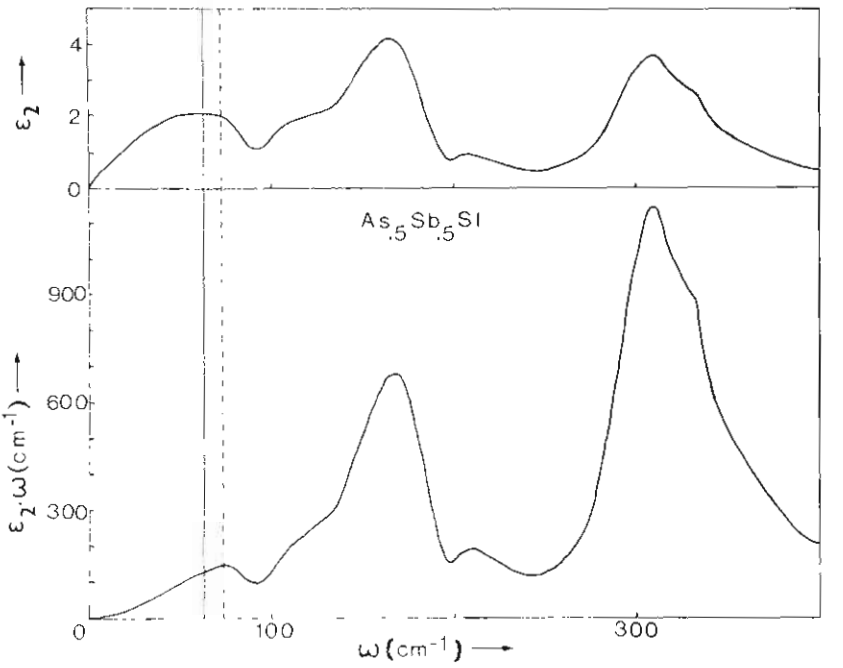


*Fig. 9. The $\varepsilon_2(\omega)$ and $\omega\varepsilon_2(\omega)$ spectra of $As_{.5}Sb_{.5}SI$ derived from K-K analysis of refleetivity data. (Unpublished data).*

with the infrared derived quantity (IR conductivity, $\sigma = \omega\varepsilon_2$)

$$\omega\varepsilon_2(\omega) \sim \sum_b D_b(\omega)\, g_b(\omega) \tag{10}$$

where the coupling coefficients $c_b^p$ and $D_b$ with which one must multiply $g_b(\omega)$ to obtain the IR and Raman spectra can be strognly frequency dependent and different for both cases.

Galeener and Sen extension of Shuker and Gamon results from Raman to Infrared responce relates the first-order Raman and IR spectra of an amorphous solid to a common set of vibrational densities of states $g(\omega)$.

Galeener and Sen [24] have also remarked that while $\omega\varepsilon_2$ is the appropriate measure of the response of the amorphous system to transverse electromagnetic wave, the quantity $-\omega\mathrm{Im}(1/\varepsilon)$, (IR resistance), is the analogous measure of response to longitudinal wave. Fig. 28 and Fig. 29 illustrate the comparison of Raman, TO- and LO- IR re-

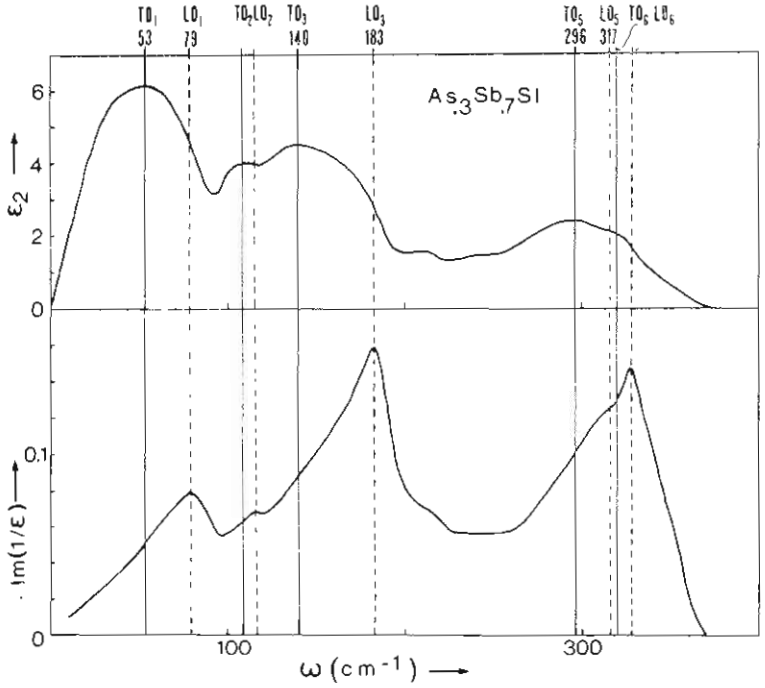


*Fig. 10. LO-TO splittings in the vibrational speetra of $As_{.5}Sb_{.5}SI$ derived from K.K analysis of reflectivity spectra. (Unpublished data).*

sponse for the vitreous SbSBr and AsSI. Similar comparison for vitreous oxides $GeO_2$, $As_2O_3$ and $As_2S_3$ and $As_2Se_3$ are reported in ref. (25).

## 5. INFRARED ABSORPTION AND REFLECTIVITY DATA ANALYSIS.

The IR-absorption $\alpha(\omega)$ can be approximated by an expression of the form

$$n\alpha(\omega) = \pi^2(4\pi Ne^2/\overline{M})\, f(\omega)\, g(\omega) \qquad (11)$$

where $f(\omega)$ is an oscillator strength that includes the frequency dependence of the matrix-elements, N is the density of atomic oscillators, $\overline{M}$ is an oscillator mass and n is the index od refraction. If $f(\omega)$ is slowly varying, then $\alpha(\omega)$ reflects the general features in the density of states $g(\omega)$. If the IR-absorption and reduced Raman spectra are very

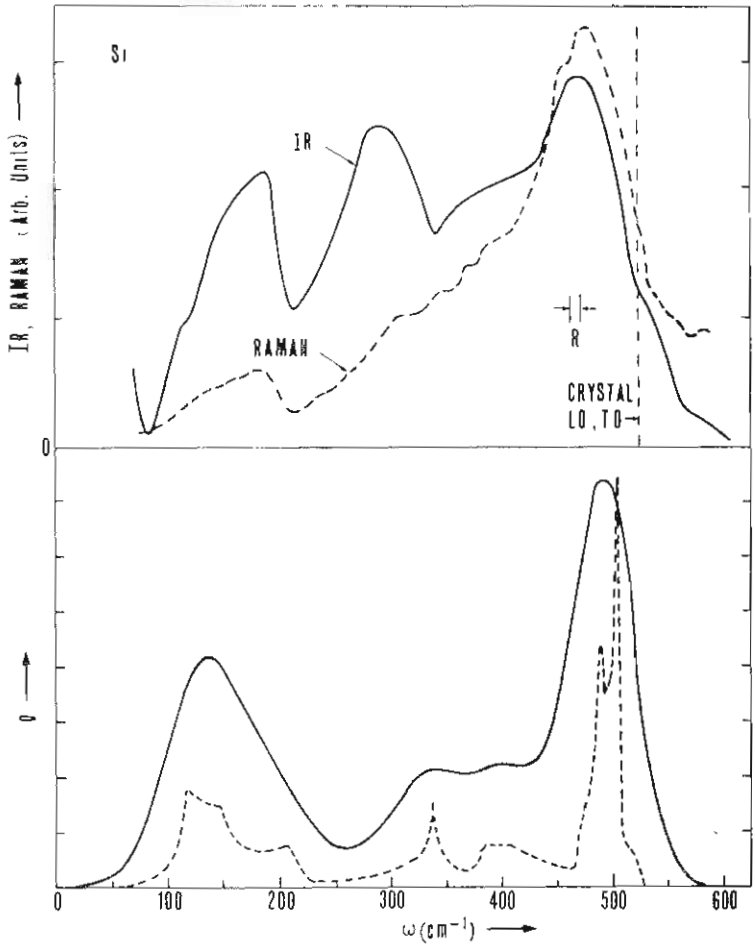


*Fig. 11. Top: Infrared absorption and reduced Raman spectrum of amorphous Si. Bottom: Density of states (dashed line) of crystalline Si from Neutron scattering data. The solid line is the crystalline density of states broadened by a convolution with a Gaussian factor of half width 25cm⁻¹. [20-22].*

different, then it can be assumed that f(ω) and its Raman counterpart are strongly frequency dependent and that matrix-element effects dominate. The bond-stretching modes, the highest frequency bands in the spectrum, generally yield the most direct structural information since their frequencies are determined primarily by nearest neighbour interactions and their relative IR or Raman acrivity by the local molecular symmetry.

The first-order IR-absorption in the elemental amorphous semiconductors is comparatively weak [$\alpha(\omega) \sim 2 \times 10^2$ cm$^{-1}$] so that transmittance spectroscopy using relatively thick films, or bulk glasses is very convenient method. As a consequence of this weak IR-activity, the index of refraction n is essentially constant over the frequency range of the IR-absorption. This means that the imaginary part of the die-

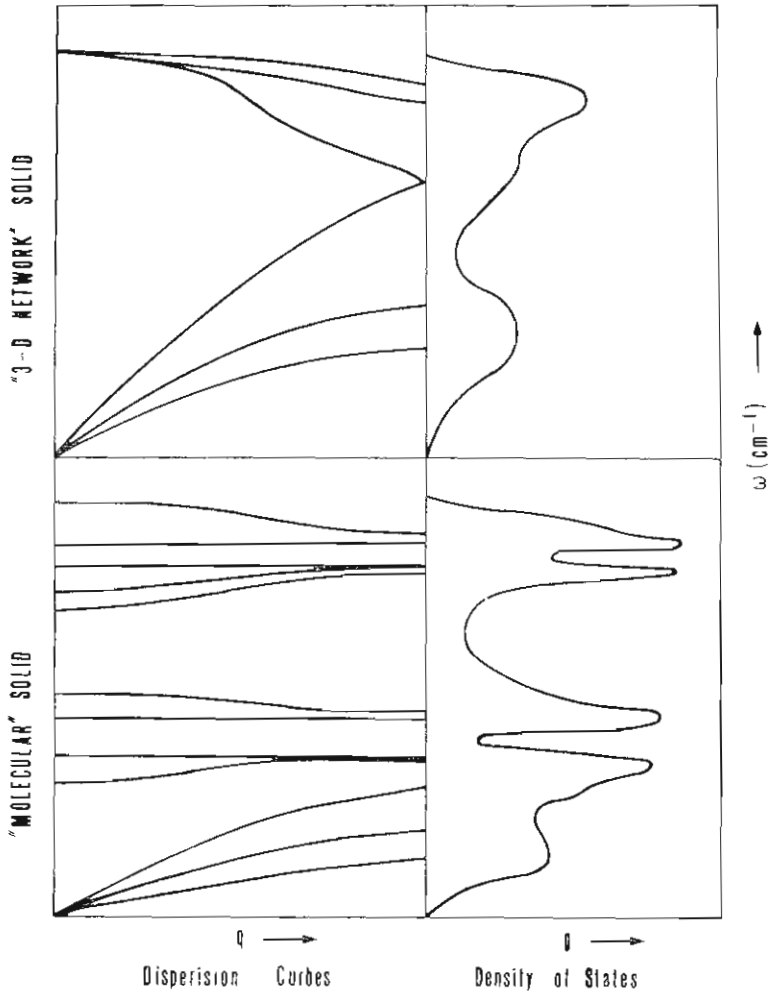


*Fig. 12. Schematic illustration of the dispersion curves (left) and vibrational density of stages g(ω) (right) for elemental tetrahedrally coordinated amorphous semiconductor (3-D.Network) top, and elemental amorphous chalogens ameneable to analysis by molecular interpretation, bottom.*




*Fig. 13. Raman*

lectric functio
frequency dep
in the case of

In contras
ger, [$\alpha_{max}(\omega)$
tice reflection
than the corr
The real $\varepsilon_1(\omega$

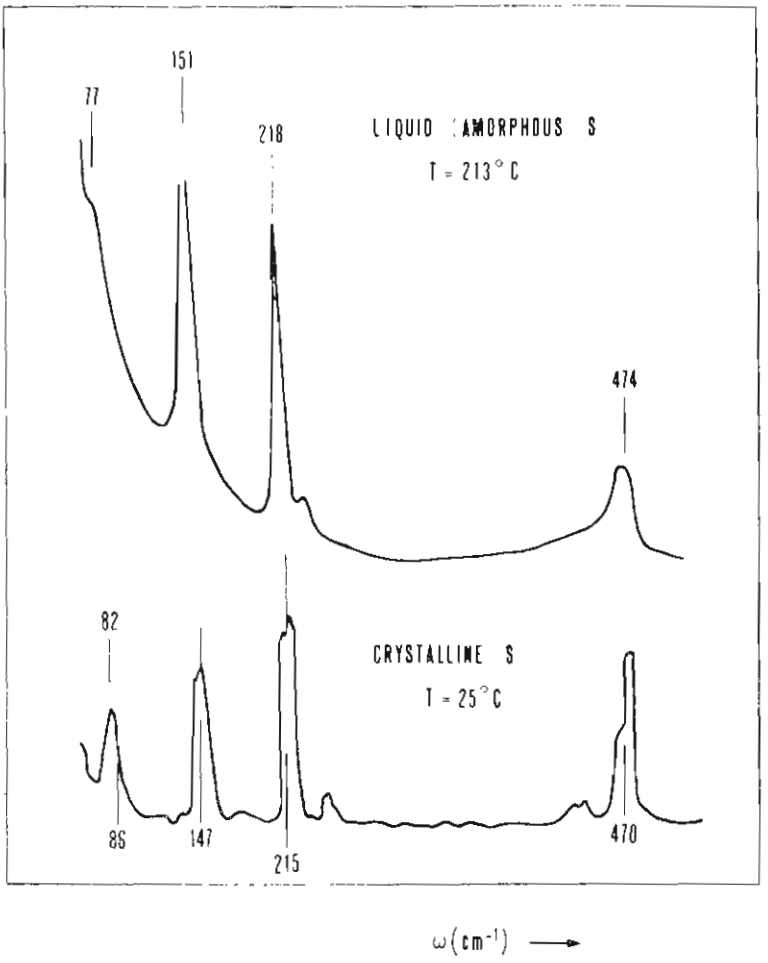


*Fig. 13. Raman spectra of crystalline and amorphous (liquid) sulfur at 25°C and 213°C respectivelly. [45].*

lectric function and the energy loss function $-\mathrm{Im}(1/\varepsilon)$ have the same frequency dependence and it is not observed any LO-TO splitting as in the case of molecular crystals.

In contrast, the IR-activity in the compounds is significantly stronger, $[\alpha_{max}(\omega) \sim 10^4 cm^{-1}]$ so that these materials exhibit observable lattice reflection bands whose analysis provides much more informations than the corresponding IR-absorption spectra but is time consuming. The real $\varepsilon_1(\omega)$ and the imaginary $\varepsilon_2(\omega)$ parts of the complex dielectric

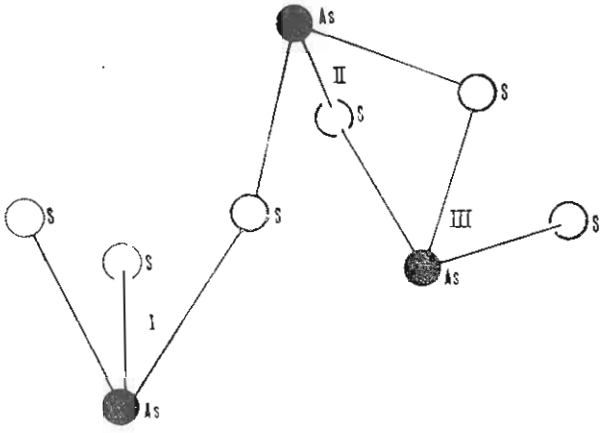


*Fig. 14. Schematic representation of the molecular structure of $As_2S_3$. The "molecule" is $AsS_{3/2}$ with bridging S atoms. Three $AsS_3$ molecules are indicated (I, II, III) in a network configuration [47].*

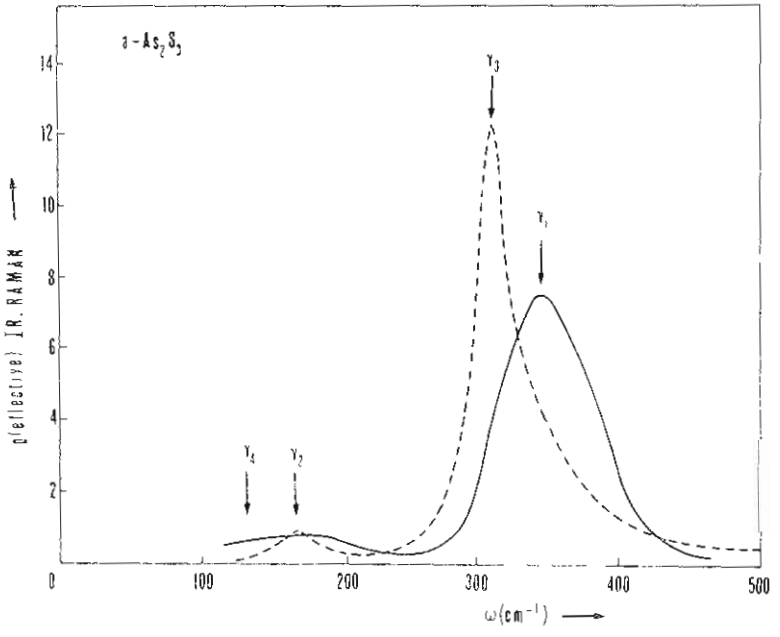


*Fig. 15. A comparison of the reduced Raman spectrum (solid line) of amorphous $As_2S_3$ with the IR absorption spectrum (dashed line) $\omega^2.\varepsilon_2$ which also has been used as effective density of states. [46].*

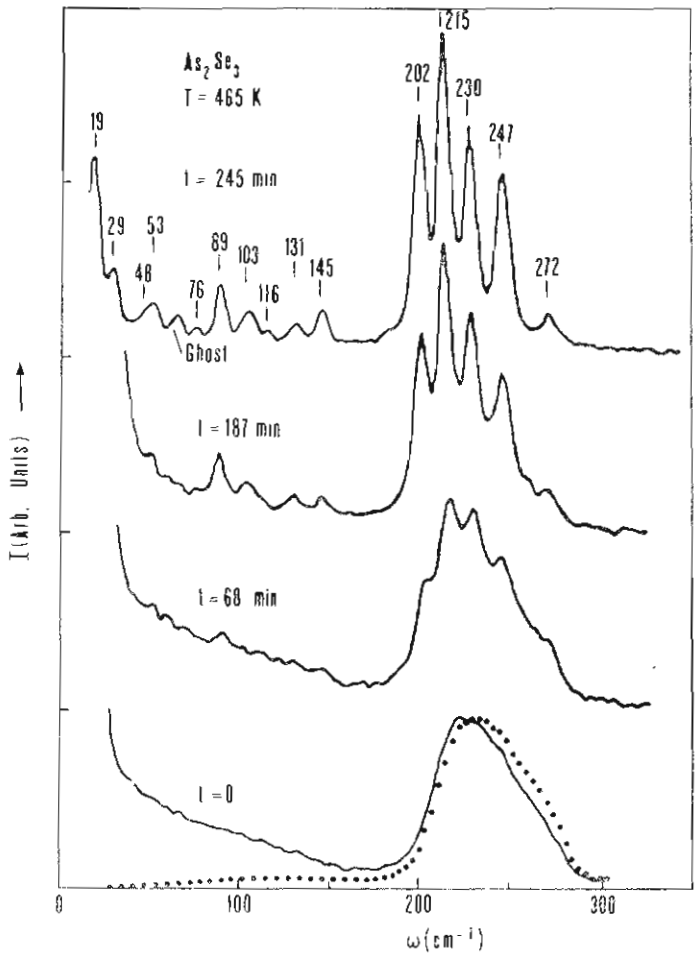


*Fig. 16. Changes in the Raman spectrum of $As_2Se_3$ during crystallization [50].*

function $\varepsilon^*(\omega)=\varepsilon_1+i\varepsilon_2$, the energy loss function, the IR-conductivity and IR-resistance and the optical constants $\alpha(\omega)$, $n(\omega)$, $k(\omega)$ can be obtained, as in the case of crystals, by Kramers-Kronig [25-27] analysis or by fitting the spectrum with some oscillator model. Lucovski et al. [28] have fitted successfully the reflectivity spectra of $Ge_{.3}S_{.7}$ glass with independent Lorentzian oscillators, but Bishop et al. [29] and Taylor, et al. [30] reported that the reflectivity spectra of $Th_2SeAs_2Te_3$ glass and $As_2Se_3$ glass are not well approximated by the Lorentzian shape which is usually observed in crystalline materials. They adopted

a fitting scheme which assumes a Gaussian (with half width $\Gamma$) distribution of Lorentzian (with half width $\gamma$) oscillators. This is the simplest statistical model which is consistent with a disordered structure. It seems that for narrow bands ($\Gamma \gg \gamma$) the line shape is Gaussian in the central region (Fig. 8, $As_2Se_3$, Se) but for $\gamma \gg \Gamma$ this model yields a Lorentzian line shape (Fig. 8, $SiO_2$). We have been always able to fit the reflectivity spectra of several $A^{V}B^{VI}C^{VII}$ glasses with Lorentzian oscillators, with the same success as the spectra of the corresponding crystals $A^{V}B^{VI}C^{VII}$ but it is true that all the bands are overdamped or heavily damped.

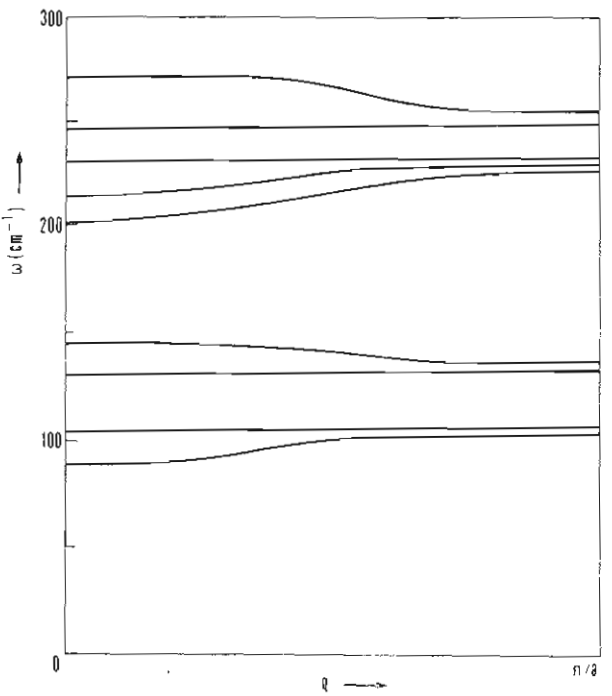


*Fig. 17. Schematic dispersion relation for $As_2Se_3$. [50].*

Provided that the reflectivity spectrum is "complete" and of high accuracy, the most convenient approach is the Kramers-Kronig analysis because these integrals are model independent as they have been derived from a causality argument. But the peaks in the $\varepsilon_2$-spectrum and energy loss spectrum correspond to the frequencies $\omega_T$ and $\omega_L$ of the vibrational modes, with transverse or longitudinal character re-

spectively, only for a classical harmonic oscillator. Moreover for a heavily damped mode the peaks of the real part of conductivity spectrum $\sigma(\omega) = \omega.\varepsilon_2(\omega)$ will correspond more closely to the $\omega_T$ than the peaks of the $\varepsilon_2$-spectrum [31] again only for a classical oscillator. In Fig. 9 it can be seen that all the higher frequency peaks of the spectra $\varepsilon_2(\omega)$ and $\omega\varepsilon_2(\omega)$, derived from K-K analysis of the reflectivity spectra of $As._5Sb._5SI$, coincide but for the lowest frequency heavily damped mode the corresponding peaks are shifted about 15% while the experimental error for $\omega_T$ is 1-2%. According to Galeener and Sen [24] the quantity $\omega.\varepsilon_2(\omega)$ is to be contrasted with the reduced Raman spectrum although most of the experimentalists [25] use the IR quantity $\varepsilon_2(\omega)$ which line shape is quite different from that of $\omega.\varepsilon_2(\omega)$ (Fig. 9).

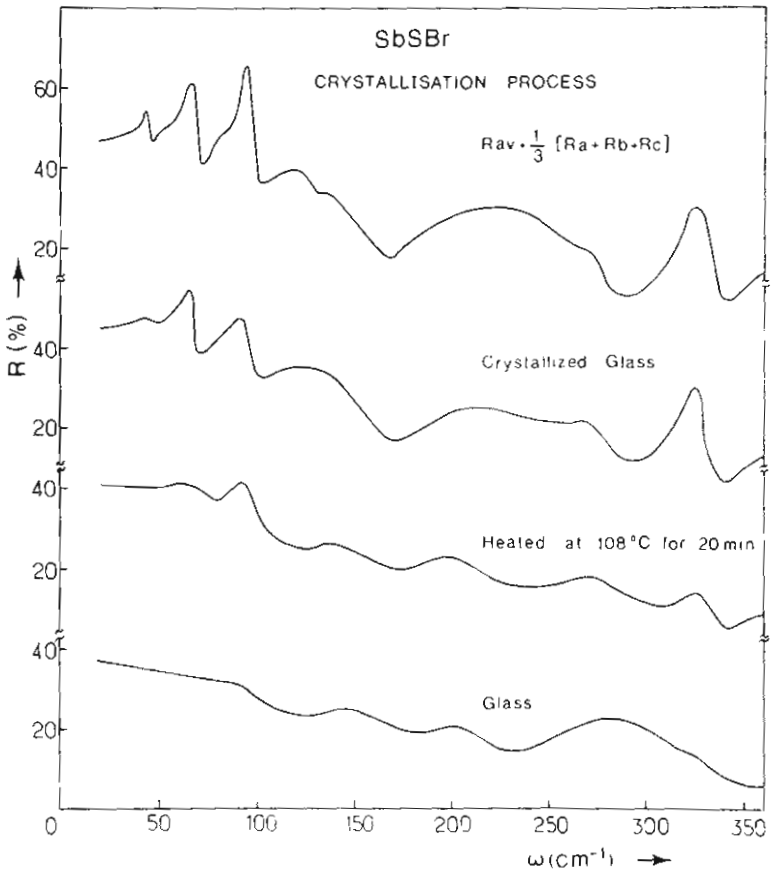


*Fig. 18. Crystallization process of SbSBr glass. [33].*

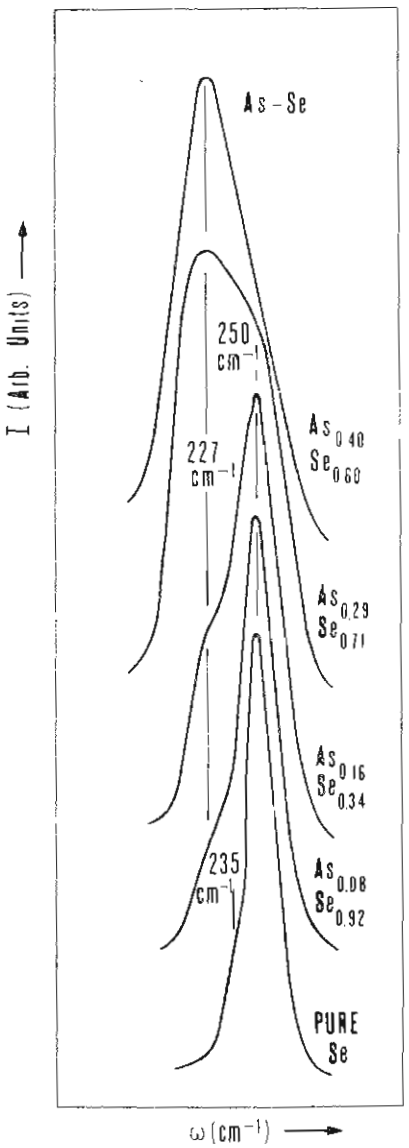


*Fig. 19. Raman spectra of binary As-Se alloy. [51].*

Another interesting aspect of vibrational spectroscopy is the recently observed large LO-TO splitting of high-frequency modes of the tetrahedral glasses [26,25] and of the lowest frequency mode of the $A^{V}B^{VI}C^{VII}$ glasses [32-34]. The order of splitting $(\omega_L-\omega_T)/\omega_T$ is $\sim 20\%$

for the oxides and ~ 50% for the $A^{V}B^{VI}C^{VII}$ (Fig. 10). This splitting leads to features in the Raman spectra [35-36] of the compounds (Fig. 28 and Fig. 29) with have been the cause for some confusion and error in earlier interpretations of the spectra. Sometimes these modes have been ascribed to unidentified impurities, or defects, or have been the reason for postulating unnecessarily complex structures for the glass. It also follows that long-range Coulomb forces should be included in complete theories of the vibrational properties of glasses.

## 6. INTERPRETATION OF IR AND RAMAN SPECTRA. MODELS

For elemental materials, it is appropriate to compare the features in the absorption spectrum, $\alpha(\omega)$, directly with the polarized Raman response. In the tetrahedrally bonded amorphous semiconductors (Ge, Si) the $\alpha(\omega)$ and the Raman spectra display only small differences in their relative weighting. In both Se and As, the differences between the IR and Raman response are more pronounced indicating a more molecular character.

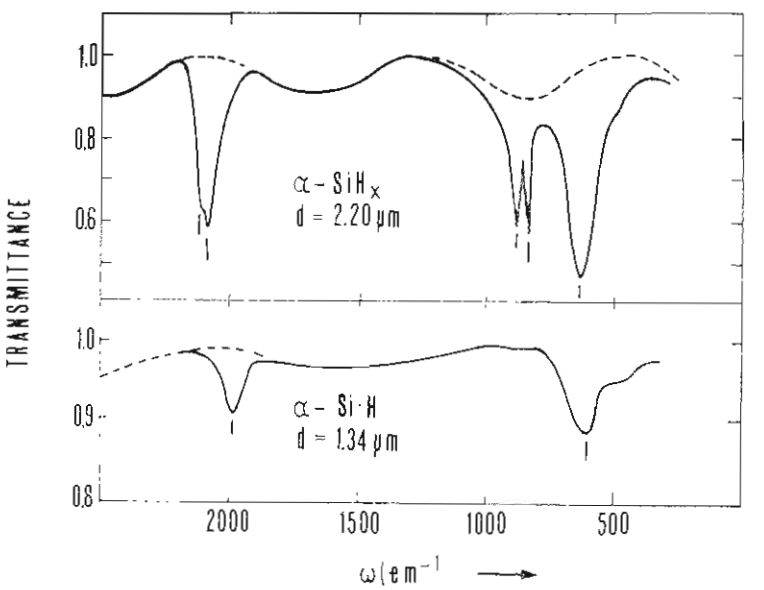


*Fig. 20. IR transmission spectra of the two types of films deposited from glow discharge plasma of silane. The upper speetrum is characteristic of a cross-linked polymerie amorphous silicon hydride (a-SiH$_x$). The lower spectrum is typical of a network of Si atoms with monohydride sites (a-SiHx). f52].*

For the compounds the IR and Raman spectra are characteristically very different. Features in the depolarization spectrum are also much sharper. It is therefore necessary to compare four spectra $\varepsilon_2$, $-\mathrm{Im}(1/\varepsilon)$, the reduced polarized Raman and the depolarization in order to provide a proper structural interpretation of the vibrational modes.

Four categories of models have been used to provide a structural basis for the interpretation of the IR and Raman spectra.

I. Models based on comparison between the vibrational spectra of crystalline and amorphous solids of the same composition [20,37].

II. Calculations based on very large clusters containing hundreds of atoms [38].

III. Calculations based on smaller clusters [39] but "properly" terminated as for example in the cluster-Bethe-Lattice method [40].

IV. Calculations based on local molecular clusters that are assumed to be vibrationally decoupled from other molecular clusters in the solid [41,42,43]. The application of local cluster models to compound systems must be done with care. It is quite possible, even though two amorphous solids like $GeS_2$ and $GeO_2$ may have very similar local atomic structure, here $GeX_{4/2}$, tetrahedra, aspects of the network connectivity can play an important role in determining the details of the IR and Raman response [43,44].

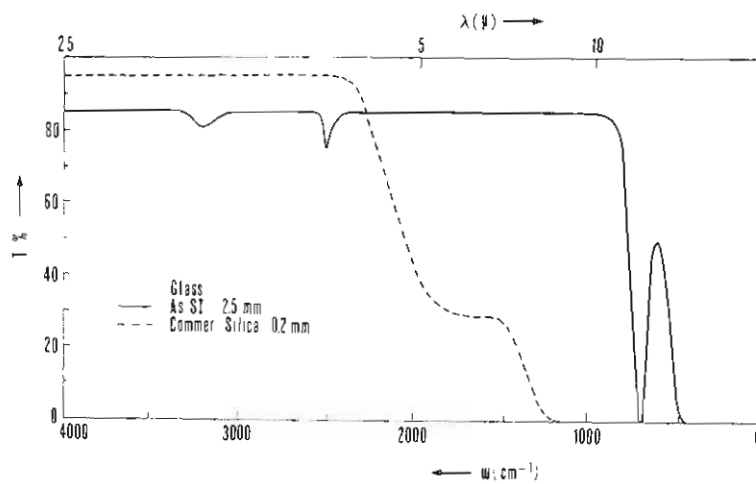


*Fig. 21. IR transmission spectra of AsSI glass in comparison to a commereial silica glass. [Unpublished data].*

## 7. TETRAHEDRALLY BONDED AMORPHOUS SEMICONDUCTORS

Amorphous Si [20-22] and Ge [21-23] have been studied as the prototype of the tetrahedrally coordinated semiconductors. There are two general and important physical implications that can be drawn from the experimental IR-absorption and Raman spectrum of either amorphous Si (Fig. 11) or Ge.

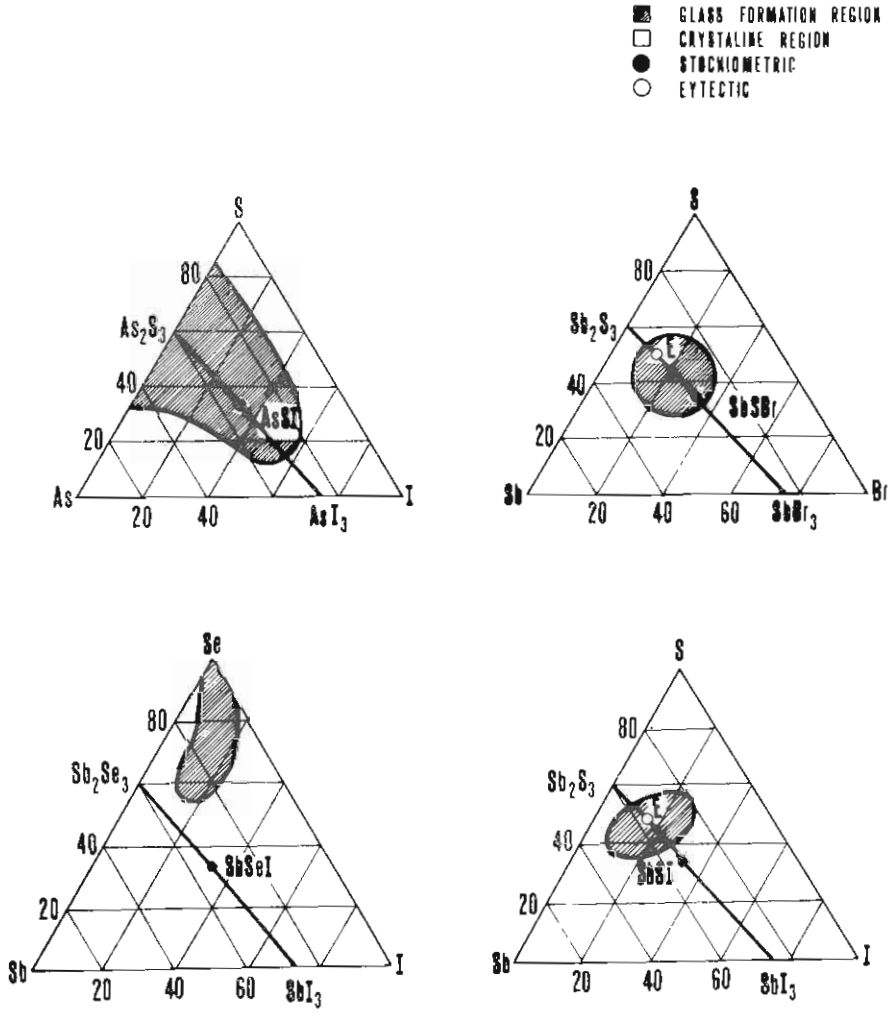


*Fig. 22. The phase diagrams of glass formation in several AVBVICVII systems: AsSI [59], SbSI [57], SbSBr [53], SbSeI [58].*

(I). The first-order IR and Raman spectra cover the entire vibrational energy range whereas for the corresponding crystal state only one zone center optical phonon is Raman active and non Infrared.

(II). Not only the observed IR and Raman spectra show the gross features of the entire amorphous vibrational density of states, but the amorphous density of states is very similar to that of the corresponding crystal modified by matrix element effects. This confirms that for Si the crystalline SRO is carried over to the amorphous form.

Raman and IR spectra of the amorphous III-V compounds GaAs [22-23], GaP habe been reported by several groups. To ascertain extent, the basic results of the Si and Ge are carried over to the III-V compound.

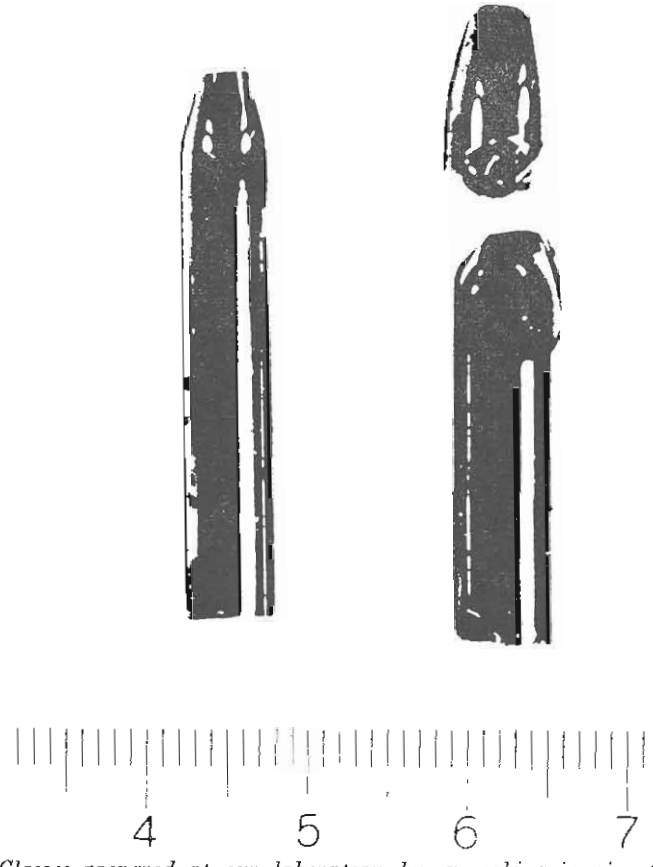


*Fig. 23. Glasses prepared at our laboratory by quenching in air stoiehiometric SbSBr melt.*

## 8. AMORPHOUS CHALCOGENS AND CHALCOGENIDES

Amorphous chalcogenides are of interest because, among other phenomena, there are many photoelectronic and photostructural effects special to this class of semiconductors. Some aspects of the vibrations in amorphous chalcogenides are interpretable in terms of the general features of disorder induced activity of a broad density of states, as in the case of the tetrahedrally bonded semiconductors. However, much of the vibrational motion can be associated with "molecular" units which are in some sense decoupled from the rest of the amorphous network. Localized modes imply flatter dispersion curves and consequently sharper features in the density of vibrational states. The difference between the broad spectra of tetrahedrally interconnected semiconductors and most of the lower coordinated chalcogenides is illustrated in Fig. 12.

Elemental rhombic sulfur is composed of puckered 8 atoms rings ($S_8$) which are the molecular units. Fig. 13 shows Raman spectra of Ward [45] for crystals at 25°C and liquid (amorphous) S at 213°C.

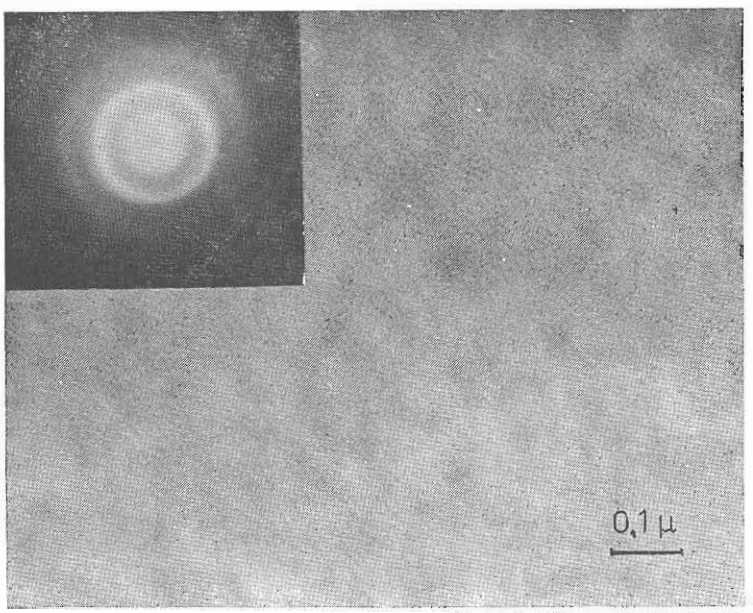


*Fig. 24. Eleetron-diffraction halos and bright field micrographs obtained by Transmission Electron Microscope examination to confirm the amorphous state of SbSBr glass (The photograph has been taken by E. Polychroniadis).*

The crystal vibrational modes with frequencies above about 75 $cm^{-1}$ are intramolecular and are clearly preserved with some broadening, but with little if any frequency shifts in the liquid. Thus sulfur is an "ideal" example of the molecular case.

Consider next the simple chalcogenide compound $As_2S_3$ which can be prepared in the bulk form by quenching the melt. The information that is readily obtainable from an interpretation of their IR and Raman spectra relates to two aspects of the local atomic structure:
I. The distribution of heteropolar and homopolar bonds.
II. The symmetries of the local atomic clusters (Fig. 14).

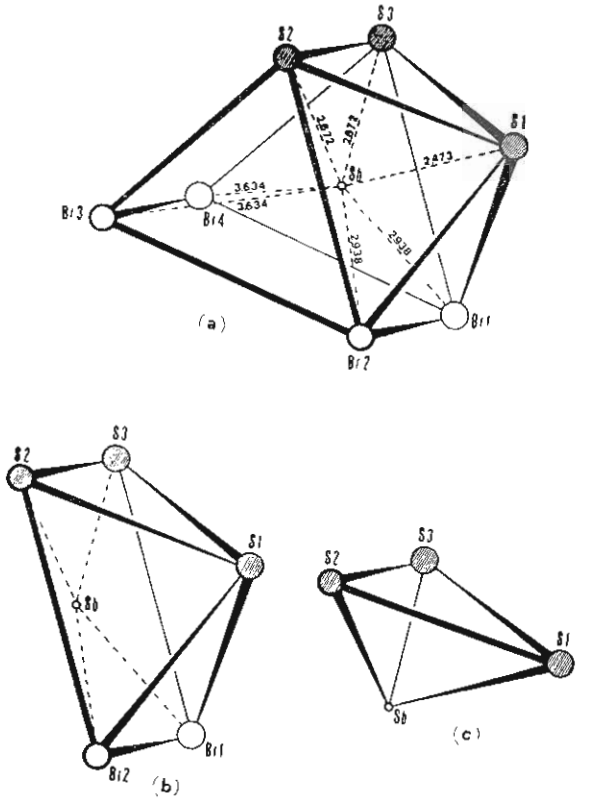


*Fig. 25. (a) The coordination polyhedron of SbSBr for the full unit shell of* $D_{2h}^{16}$ *space group [65].*

*(b) Schematic picture showing the shape (double square pyramid) of SbSBr molecule in the simplified unit shell (SUC) of* $C_{2h}^{2}$ *spaee group.*

*(e) Another "moleeular unit" a trigonal pyramid, formed only by the three Sb-S bonds mueh stronger than the Sb-*$Br^{(1)}$ *and Sb-*$Br^{(2)}$ *bonds.*

Fig. 15 displays the IR and Raman spectra for $As_2S_3$ [46]. The dominant features in the $\varepsilon_2$ and Raman spectra occur in two distinct frequency regimes separated by a region of relativaly low optical activity. The features in the high frequency regime, $\omega > 300$ cm$^{-1}$ are assigned to vibrational modes characterized by bond-stretching motions, while those in the low frequency regime $\omega < 200$ cm$^{-1}$ are bond-bending in character. A second important aspect of the spectra relates to the complementary activity (IR, Raman) of the bond-stretching vibrations. This type of behaviour is indicative of strong matrix elements effects, or alternatively of a spectrum that is molecular in character [47]. The same features are also present in the spectra of $GeS_2$ [48]. The simplest model for the bond-stretching modes is then based on the same molecular clusters that characterize the network structure, $AsS_{3/2}$ for $As_2S_3$ glasses (Fig. 14) and $GeS_{4/2}$ for $GeS_2$ glasses [47]. The model yields the complementary IR and Raman activity. The success of the molecular model for the bond-stretching modes is due to an effective decoupling of these modes at the two-fold coordinated S atom-sites. The coupling

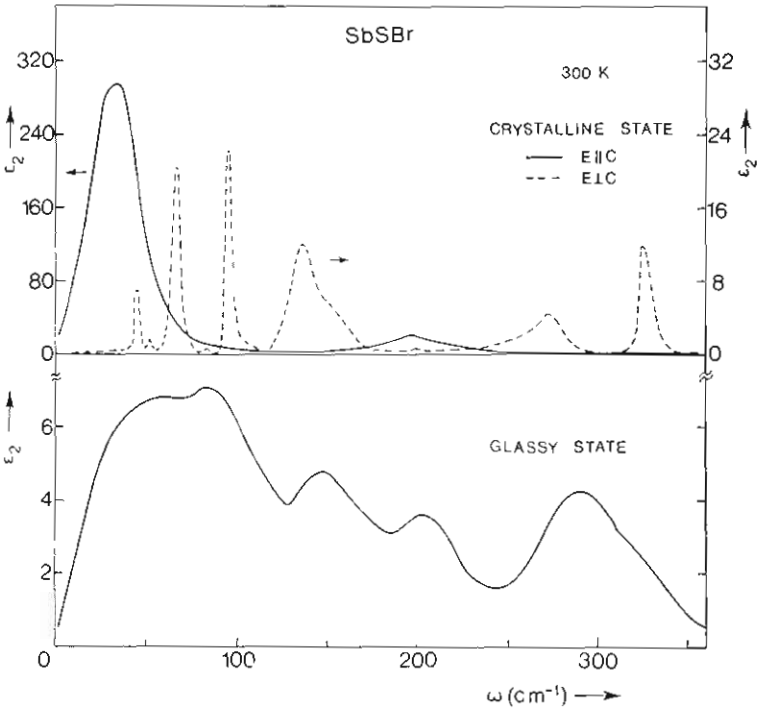


*Fig. 26. The $\varepsilon_2$-spectrum of SbSBr crustal and glass derived from Kramers-Kronig analysis of the IR-reflectivity spectrum. [33].*

is small due to the near 90° bond angle at the S-atom sites, (Fig. 14) as is demonstrated in the model calculations of de Fonzo and Tauc [41] and Sem and Thorpe [42].

Another important aspect is that the dominant vibrational peaks in $As_2Se_3$ still exists not only above $T_g$ ($\sim 460\,^0K$) but also above the melting point ($633\,^0K$) for crystalline $As_2Se_3$ [49]. As for $As_2Se_3$, the dominant bands observed in amorphous Se persist in the liquid state indicating again the preservation of molecular like units in this state.

## 9. LASER ANNEALING AND REAL TIME RAMAN SCATTERING

The study of crystallization of amorphous materials by using real time Raman scattering finds extensive application nowdays [12]. The recrystallization of $As_2Se_3$ has been studied by Finkman et al. [50]. $As_2Se_3$ is an extremely stable glass and does not normally crystallizes in the dark even at temperatures above the glass transition $T_g \simeq 460\,^0K$. The illumination was provided by the same incident laser beam (5145 Å

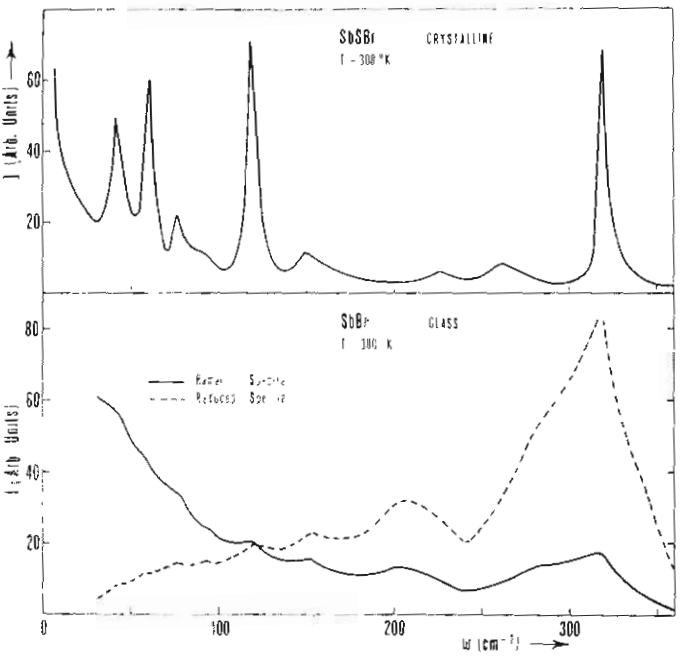


*Fig. 27. The measured and reduced Raman spectra of SbSBr in the crystalline and amorphous state. [35].*

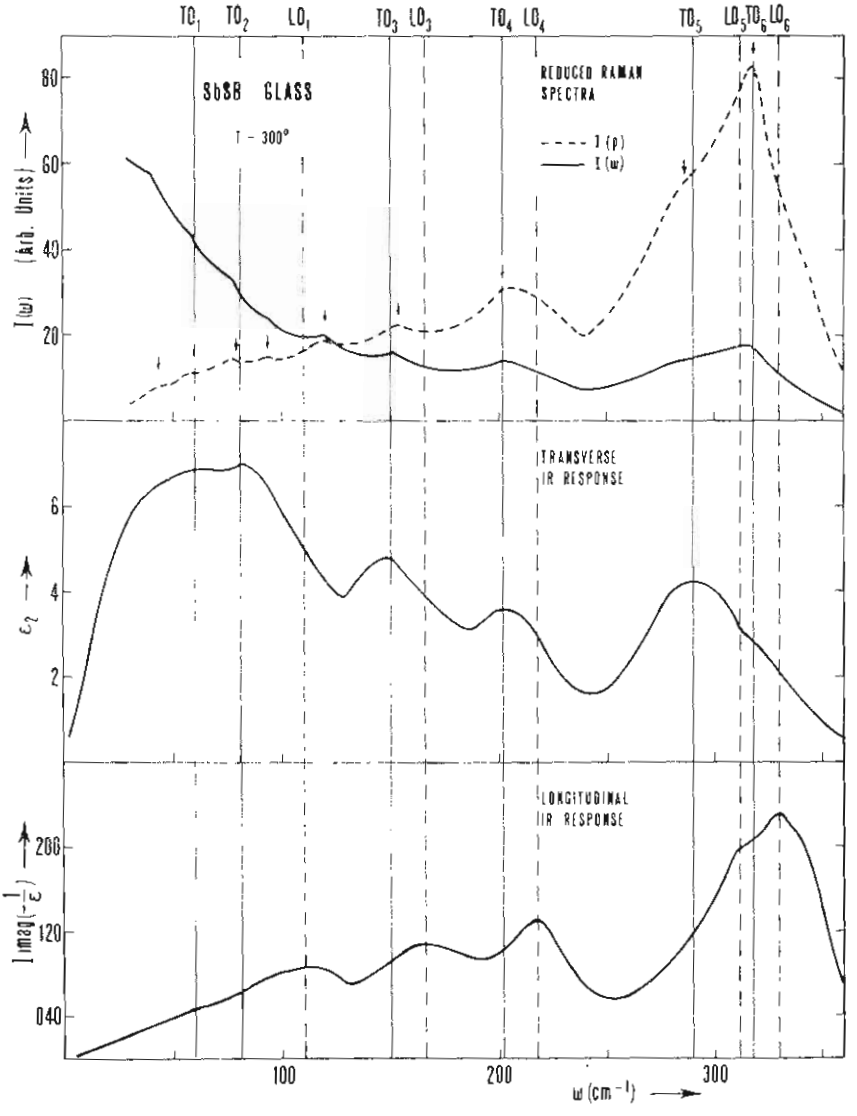


*Fig. 28. Transverse and Longitudinal IR response (derived from K-K analysis) in comparison to Raman response of SbSBr glass. The eomplementary aetivity of IR and Raman is indicative of strong matrix element effeets. [35].*

argon line) used for the scattering measurements. Fig. 16 shows that the Raman spectrum gradually converts in time from that of amorphous $As_2Se_3$ to that of crystal $As_2Se_3$. Finkman et al. [50], by examination

of the shift in the weight of the spectrum of Fig. 16 deduced the despersion curves of crystal $As_2Se_3$ shown schematically in Fig. 17. Recently we have studied [33] the size dependence of ferroelectric behaviour during the crystallization process, heating the vitreous SbSBr, for gradually increasing time intervalls, at temperatures above the crystallization temperature $T_{cr} = 108^{o}C$. In Fig. 18 it is shown that during the crystallization the IR spectrum gradually converts from that of the amorphous SbSBr to the average reflectivity spectrum $R_{av} = 1/3[R_c + 2(R_{a+b})]$ of the single crystal for polarizations E//c and E⊥c and that the hard "ferroelectric" mode softens while its strength increases.

## 10. BINARY ALLOYS

Vibrational spectra have proven to be a particularly useful tool in studying the local atomic structure in binary alloy systems and two examples are given below.

### *10.1 As-Se alloy*

The general motivation for study of the amorphous chalcogens and their compounds and alloys has been technological. Xerox's interest in amorphous sulfur and selenium dates back to 1938 when Chester Carlson first demostrated the phenomenon of electrophotography. Addition of As to Se increased the glass transition temperature and the stability of the vitreous phase by forming a cross-linked polymer network. Such consideration emphasized the need to confirm the microscopic origins of physicochemical correlations, and thus, far-infrared and laser Raman spectroscopy were activated [51]. In Fig. 19 it is shown, as the As concentration increases, the shoulder at 239 $cm^{-1}$ in the spectrum of vitreous Se broadens, increases in intensity relative to the $Se_8$ peak at 250 $cm^{-1}$, and shifts to lower energy. Between 16 and 29 atomic % As the $Se_8$ rings disappear leaving only the broad spectral feature at 227 $cm^{-1}$ associated with As-Se network polymer. This is the only feature in the spectrum of $As_{0.40}Se_{0.60}$.

### *10.2 Si-H alloy*

Hydrogen is an important constituent of those forms of amorphous silicon that are currently of most interest for their photoelectronic and doping properties. Hydrogen plays a role in removing electronic states

from the semiconductor band gap, thus permitting p-and n-type dopping by trace impurities. Bonded hydrogen in either crystalline or amorphous silicon is detectable by Raman or IR spectroscopy [12]. Fig. 20 shows the IR transmittance [52] of two structurally different films of hydrogenated amorphous silicon prepared from glow-discharge plasma of silane ($SiH_4$). The occurence of other than monohydride sites has important and deterious effects on the electronic and photoelectronic properties of amorphous silicon. For example, poorer quality Schottky barrier diodes results from those deposition conditions known, by IR-spectroscopy, to increase the concentration of $SiH_2$. In extreme cases

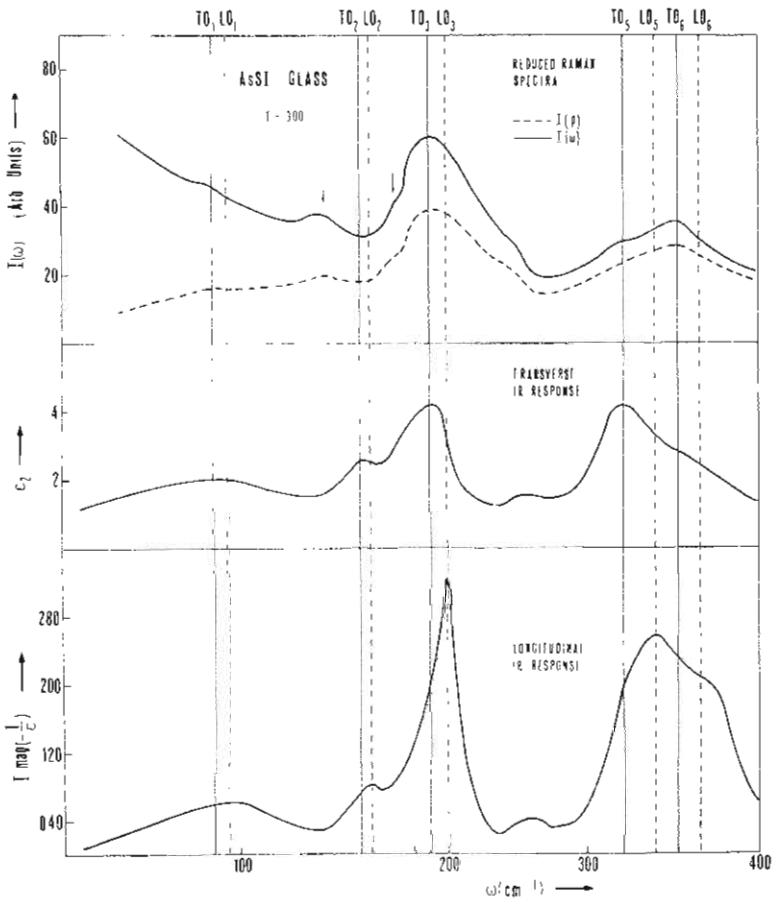


*Fig. 29. The three spectra, $\varepsilon_2$, $-Im(1/\varepsilon)$ and Raman of AsSI glass. Matrix element effects are clearly present in the high frequency bond-stretching modes. [Unpublished data].*

of predominantly di- and trihydride sites for the H, the silicon network breaks up [52] and it is no longer appropriate to refer to the material as amorphous silicon with H (α-Si:H) but rather as a hydride of Silicon (α-$SiH_x$). The upper half of fig. 20 is typical of α-$SiH_x$ while the lower half is typical of α:Si:H.

## 11. AMORPHOUS FERROELECTRIC $A^vB^{vi}C^{vii}$ COMPOUNDS.

We have said already, amorphous materials are difficult to understand and the same is also applied for the crystalline ferroelectric materials. This explains perhaps why researchers avoid to meet the problem of "amorphous ferroelectric", the influence of disorder in the soft mode and the size dependence of the ferroelectric behavior, although optical lattice vibrational spectra have been thoroughly studied for dozens of ferroelectric crystals. The whole area has been left virgin at the last 4th European Meeting on Ferroelectricity (Portoroz, 1979) where among three hundred contributions only one paper [33] was concerned to this

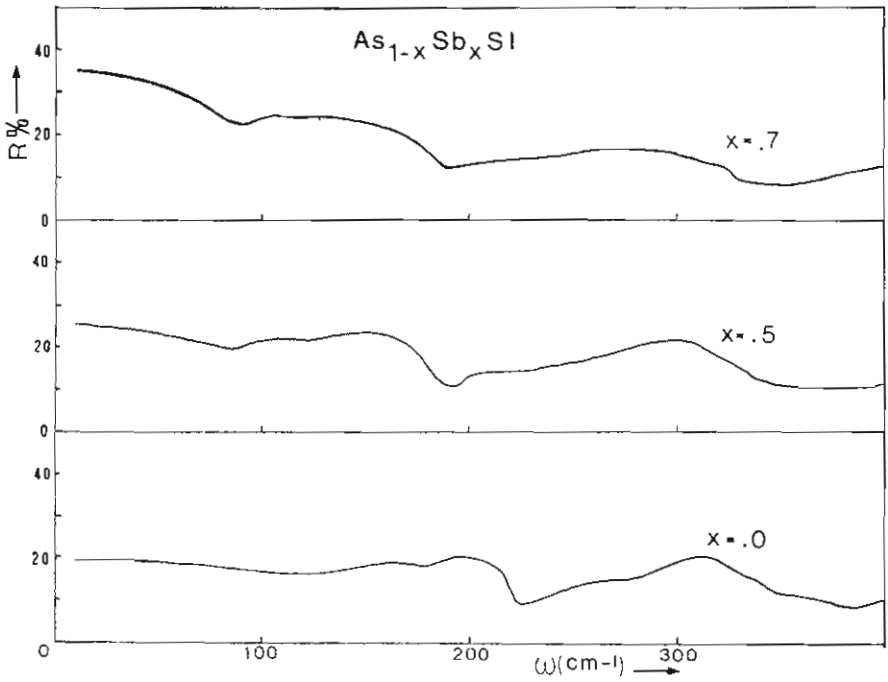


*Fig. 30. IR-reflectivity spectra in the pseudobinary alloy amorphous system* $[AsSI]_{1-x}$-$[SbSI]_x$. *[Unpublished data].*

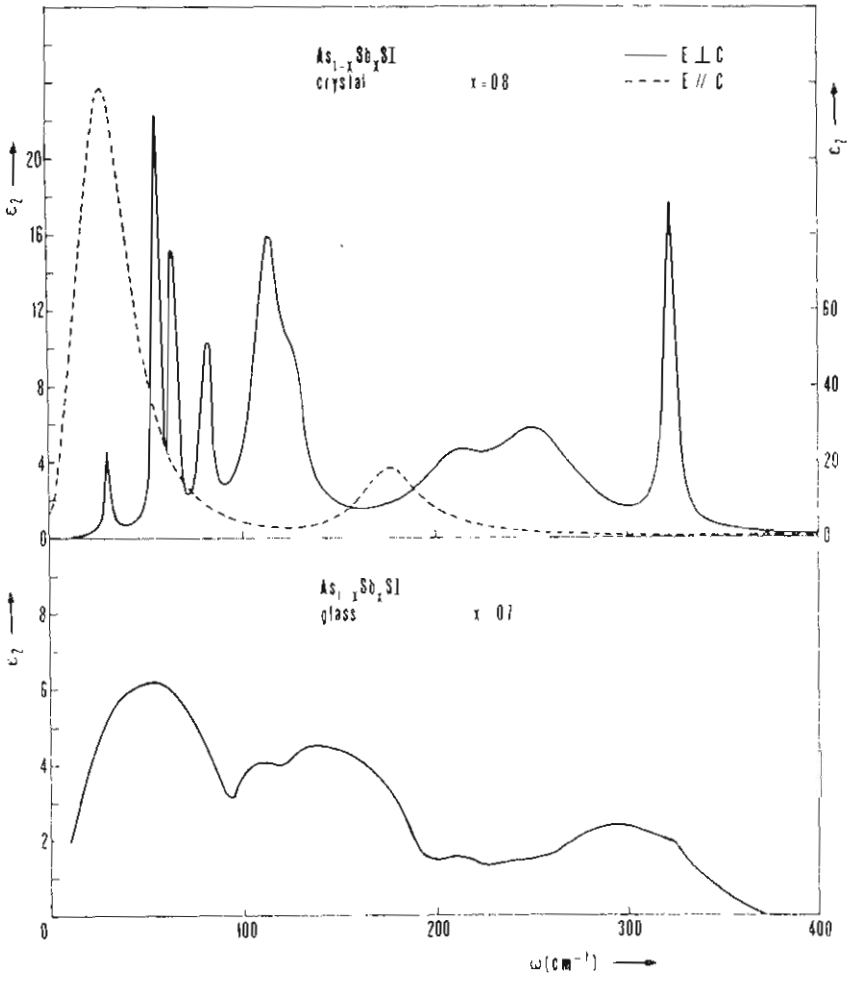


*Fig. 31. Comparison of the infrared $\varepsilon_2$-spectrum in the crystalline ($x$= .8) [64] and amorphous ($x$=.7) form of the system $[AsSI]_{1-x}$-$[SbSI]_x$.*

subject, reporting for the first time on the vibrational properties of a ferroelectric compound (SbSBr) at the transition from crystalline to vitreous phase. It has only recently been shown that glasses of the ferroelectric materials SbSBr [53] [32], $LiNbO_3$ and $LiTaO_3$ [54] and $Pb_5Ge_3O_{11}$ [55] can be formed directly by water or air quenching a melt. Also recently the concept of a ferroelectric glass was explored and there was found no fundamental objection to the concept [56].

It is very attractive to fabricate glasses of $AsB^{VI}C^{VII}$ (e.g. AsSI, AsSBr) and $SbB^{VI}C^{VII}$ (e.g. SbSI, SbSBr) semiconductive ferroelectric compounds from the point of view of optoelectronic applications utilizing their many interesting properties which otherwise cannot be used because of the technical difficulties in growing large crystals. Moreover due to their very high IR transmittance (in comparison to oxide glasses, Fig. 21) and low $T_g$ (in comparison to $As_2S_3$ glasses) are of considerable interest for their potential practical use in IR optics.

In Fig. 22 we have summarized the known phase diagrams of glass formation in the ternary systems $SbB^{VI}C^{VII}$ ($B^{VI} = S, Se$, $C^{VII} = I, Br$) [53], [57], [58] and $AsB^{VI}C^{VII}$. (The phase diagrams of AsSeI and AsSBr are similar to that of AsSI [59]).

Generally the glass formation is not restricted to certain kinds of materials. However the differences in the glass-forming tendency, as between the $SbB^{VI}C^{VII}$ and $AsB^{VI}C^{VII}$, are enormous. The composition of the ternary compounds AsSI and SbSBr lie within the glass-forming region but not, of the SbSI and SbSeI compounds. In the last system

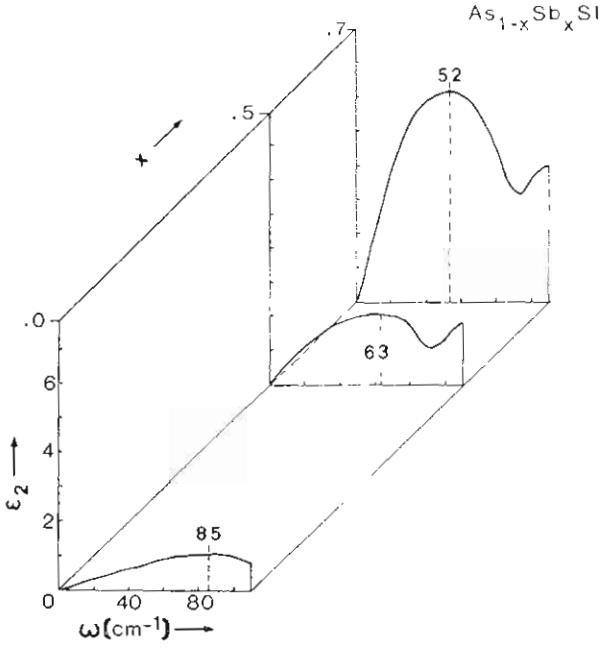


*Fig. 32. The $\varepsilon_2$-spectrum of the amorphous system $[AsSI]_{1-x}$-$[SbSI]_x$ derived from K-K - analysis of Fig. 30 reflectivity spectra, and showing softening of the local "ferroelectric" mode. [Unpublished data].*

SbSeI is not included even the eutectic point. It is so small the glass-forming tendency in the ferroelectric compounds SbSI and SbSeI that even when we cool very small quantities (~1-2gr.) of stoichiometric melt quickly, by plunging the quartz capsules into liquid $N_2$, always the resulting material is crystalline. In the opposite case it is impossible to prepare crystals by cooling AsSI melt, but always glass even under the smallest possible cooling speed. In Fig. 23 are shown typical SbSBr glasses prepared at our laboratory by quenching in air stoichiometric melt. Typical signs of vitrification are metallic luster, characteristic concoidal fracture, optical uniformity when examined under the microscope in reflected light and the absence of lines in X-ray diffraction or electron-diffraction patterns. The electron diffraction halos taken in transmission Electron Microscope examination are shown in Fig. 24 together with dark field micrographs taken from the same position of the sample. No crystalline grains are observed.

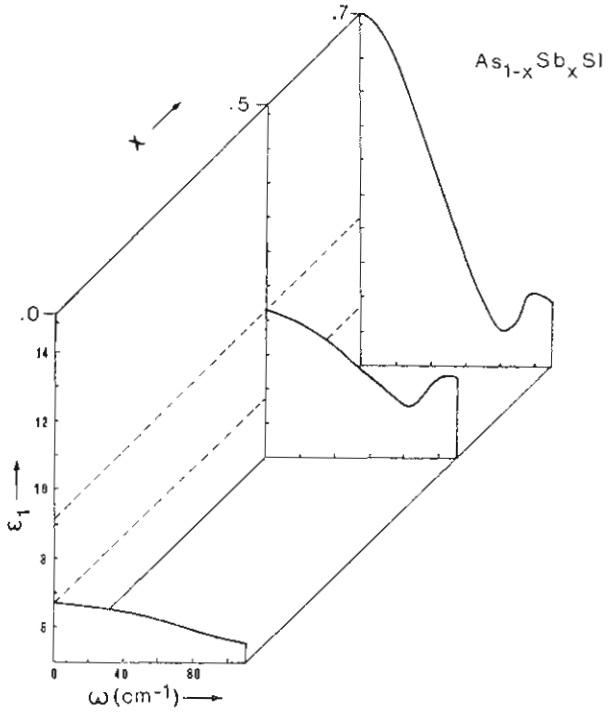


*Fig. 33. The $\varepsilon_1$-spectrum of the amorphous system $[AsSI]_{1-x}$-$[SbSI]_x$ showing strong increase of $\varepsilon(o)$ due to a strong increase of the oscillator strength $\Delta E$ of the local "ferroelectric" mode. [Unpublished data].*

The optical vibrations of the crystalline form of the most $A^{V}B^{VI}C^{VII}$ compounds, in single component crystals [60] - [62] and their solid solutions [63], [64] were studied recently. The crystals have a chain structure with $D_{2h}^{16}$ space group containing four molecules per unit cell[65]. To a good approximation one may assume a simplified unit cell (SUC) that contains only two molecules and has a symmetry of $C_{2h}^{2}$ space group. The chains are built of strongly bonded $Sb(S_2Br_2)_{1/2}$ square pyramids (Fig. 25). The amorphous form is built practically of the same pyramids. From one point of view one stresses the existence of the remnants of the chain structure in the amorphous form. From the opposite point of view, the glass is considered to be a 3-dimensional interconnected network composed of pyramidal $Sb(S_2Br_2)_{1/2}$ units. Group theory, for both the crystal SUC and the square pyramid, predicts nine Raman active modes (six Ag modes and three Bg modes) and six IR active modes (four Au and two Bu) but only four modes Raman and IR active for the trigonal pyramid $SbS_{3/2}$ analogous to $AsS_{3/2}$ in the amorphous compound $As_2S_3$ (Fig. 14). The observed number of modes in the IR and Raman spectra is in very good agreement with the prediction of molecular cluster $Sb(S_2Br_2)_{1/2}$ or remnants of chain structure. Consider first the SbSBr glass.

Figures 26, 27 display the IR ($\varepsilon_2$-spectrum) and Raman (measured and reduced spectra) for the crystal and glass SbSBr. In Fig. 28 are compared the three spectra [$\varepsilon_2$, -Im ($1/\varepsilon$), Raman] of the amorphous SbSBr. These spectra clearly show that all the dominant bands observed in crystalline SbSBr persist also in the glassy state, with rather strong broadening but small frequency shift, indicating the preservation in the amorphous state of a disordered chain structure with molecular-like vibrations of the same local structure as in the crystalline state. Only the ferroelectric mode, observed at $\omega = 35\ cm^{-1}$ in the SbSBr crystal shifts remarkably to $\omega \simeq 70\ cm^{-1}$ at the transition to the vitreous phase. The same is also observed in the IR-spectrum of crystal and glass $As_{.3}Sb_{.7}SI$ (Fig. 31). The dominant features in the $\varepsilon_2$, -Im ($1/\varepsilon$) and Raman spectra of amorphous SbSBr (Fig. 28) AsSI (Fig. 29) and AsSI-SbSI mixed glass (Fig. 30, 31) occur in distinct frequency regimes separated by regions of relatively low optical activity. The features in the high-frequency regime, $\omega > 300\ cm^{-1}$, are assigned to vibrational modes characterized by bond-stretching motions. A second important aspect of the spectra relates to the complementary activity (IR-Raman) of the bond-stretching vibrations and the lowest

frequency ferroelectric mode. This type of behavior is indicative of strong matrix element effects, or alternatively of a spectrum that is molecular in character.

Another important aspect is the observed relatively large TO-LO splitting for the highest frequency modes analogous to that reported recently [25] in several oxides ($GeO_2$, $SiO_2$) and the very large, about 50%, TO-LO splitting of the lowest frequency band (Fig. 28, Fig. 10, Fig. 31) observed for the first time. The relative high value of the static dielectric constant $\varepsilon_1(o)$, and the oscillation strength accounting for about 80% of $\varepsilon_0$ and the TO-LO splitting of the lowest frequency mode in SbSBr and $(AsSI)_x$ - $(SbSI)_{1-x}$ glasses indicate that induced dipolar interaction and long range Coulomb forces play an important role in the vibrational properties of these glasses and should be included in complete theories.

Figure 30 displays the room temperature reststrahlen IR-reflectivity bands of the mixed glasses $As_{1-x}Sb_xSI$. Kramers-Kronig analysis shows, the dominant bands display a one-mode behavior in the pseudobinary alloy system $[AsSI]_{1-x}$ - $[SbSI]_x$ analogous to that reported recently for the corresponding crystalline alloy system [64] and the $[SbSBr]_{1-x}$ - $[SbSI]_x$ system [63]. From Figures 32 and 33 it is easily seen that the substitution of As by Sb leads to a room temperature softening of the lowest mode which is the temperature dependent soft mode in the ferroelectric SbSI crystal. Its frequency at 85 $cm^{-1}$, in AsSI, shifts to 52 $cm^{-1}$ in $As_{.3}Sb_{.7}SI$ while its strength $\Delta\varepsilon$ increases from $\sim 1$ to $\sim 7.5$ accounting for about 80% of the lattice contribution to $\varepsilon$ (o). This compositional softening is well established in several ferroelectric crystals [63] but is for the first time observed in amorphous "ferroelectric".

ACKNOWLEDGEMENT

The illustration with examples of this paper is partly based on an experimental work, concerning the amorphous $A^{V}B^{VI}C^{VII}$ compounds done at our laboratory with my coleagues K. Paraskevopoulos, A. Barzokas and mainly A. Koutsoudakis and was supported by the director of the laboratory professor N. Economou.

REFERENCES


1. W. H. Zachariasen, J. Am. Chem. Soc. 54, 3841 (1932).
2. J. Zarzycki, in Physics of Non-Crystalline Solids, edited by G. Frischat, p. 52 (1977).
3. E. Porai-Koshits, in Glass Science, edited by J. Götz (North-Holland) p. 86 (1977).
4. B. Bagley, in Amorphous and liquid Semicondnctors, edited by J. Tauc (Plenum) p. 1 (1974).
5. Jr. Barker, Rev. Mod. Physics 47, Suppl. No2, 1 (1975).
6. E. Davis, in Electronic and Structural Properties of Amorphous Semiconductors, edited by P. Le Comber and J. Mort (Acad. Press) p. 425 (1973).
7. M. Brodsky, in Light Scattering in Solids, edited by M. Cardona (Springer) p. 205 (1975).
8. J. Axe, in Physics of Structurally Disordered Solids edited by S. Mitra (Plenum), NATO Advanced Study Institutes Series, Vol. 20, p. 507 (1976).
9. M. Thorpe, in Vibrational Spectroscopy of Molecular Liquids and Solids, edited by S. Bratos and R. Pick (Plenum) NATO, A.S.I.S. vol. 56, p. 341 (1980).
10. Proceedings of tbe 8th International Conference on Amorphous and Liquid Semiconductors, Cambridge, Mass., edited by W. Paul and M. Kastner (North-Holland) 1980.
11. Proceedings of the 14th International Conference on the Physics of Semiconductors, Edinburgh, edited by B. Wilson (1978).
12. Proceedings of the 15th International Conference on the Physics of Semiconductors, Kyoto, edited by Sh. Tanaka and Y. Toyozowa, 1981.
13. N. Mott, E. Davis, Electronic Processes in Non-Crystalline Materials (Oxford Univ. Press), 1971.
14. N. Onodera, H. Syga and J. Syuzoseki, J. Non-Crystalline Solids, 1, 331 (1969)
15. P. Dean, J. Inst. Maths. Applics., 3, 98 (1967).
16. R. Shuker and R. Gammon, Phys. Rev. Lett., 25, 222 (1970).
17. G. Lucovsky, Amorphous and Liquid Semiconductors, (Taylor and Francis p. 1009 (1974).
18. S. Solin, Structure and Excitations in Amorphous Solids, (Am. Inst. Physics) p. 205 (1976).
19. R. Kobliska, S. Solin, Phys. Rev. B8, 756 (1973).
20. J. Smith, et al., Phys. Rev. Lett., 26, 642 (1971).
21. M. Brodsky, Phys. Rev., B9, 1646 (1974).
22. G. Dolling, R. Cowley, Proc. Phys. Soc., London 88, 463 (1966).
23. J. Smith, et al., Light Scattering in Solids, (Flammarion) p. 330 (1971).
24. F. Galeener, P. Sen, Phys. Rev., B17, 1928 (1978).
25. F. Galeener, G. Lucovsky, R. Geis, Pbys. Rev., B19, 4251 (1979).
26. F. Galeener, G. Lucovsky, Phys. Rev. Lett., 37, 1474 (1976).
27. P. Gaskell, D. Johnson, J. Non-Cryst. Solids, 20, 153 (1976).
28. G. Lucovsky, J. de Neufrille, et al., Phys. Rev., B9, 1591 (1974).
29. S. Bishop, et al., J. Non-Cryst. Solids, 5, 351 (1971).
30. P. Taylor, et al., Sol. State Commun., 8, 1783 (1970).

31. A. Bartsokas and D. Siapkas, Ferroelectrics 25, 561 (1980).
32. A. Koutsoudakis and D. Siapkas, 6th Physics Week, Only Abstracts, p. 123, Athens 1976.
33. A. Koutsoudakis and D. Siapkas, Ferroelectrics, 25, 593 (1980).
34. D. Siapkas and C. Paraskevopoulos, Unpublished data.
35. A. Koutsoudakis and D. Siapkas, Proceedings of the 2nd Panellinio Conference of Physics, Mytilini, Greece September 1980.
36. C. Paraskevopoulos and D. Siapkas, Unpublished data.
37. R. Alben et al., Phys. Rev. B11, 2271 (1975).
38. R. Bell, P. Dean, Discuss. Faraday Soc. 50, 55 (1970).
39. M. Thorpe, Phys. Rev. B8, 5352 (1973).
40. J. Joannopoulos, W. Pollard, Solid State Commun. 20, 947 (1976).
41. A. De Fonzo, J. Tauc, Solid State Commun. 18, 937 (1976).
42. P. Sen, M. Thorpe, Phys. Rev. B15, 4030 (1977).
43. F. Galeener, Phys. Rev. 19B, 4292 (1979).
44. R. Laughlin and J. Joannopoulos, J. Phys. Rev. B16, 2942 (1977).
45. A. Ward, J. Phys. Chem. 72, 4133 (1968).
46. G. Lucovsky, Phys. Rev. B6, 1480 (1972).
47. G. Lucovsky and R. Martin, J. Non-Crystalline Solids, 8 - 10, 185 (1972).
48. G. Lucovsky et al. Phys. Rev. B8, 5947 (1973).
49. P. Taylor et al. Phys. Rev. Let. 27, 414 (1971).
50. E. Finkman et al. Proceed. 12th Intern. Confer. on the Physics of Semicondutors Stuttgart, 1022 (1974).
51. A.Ward, Advan. in Chem. 110, 163 (1972).
52. M. Brodsky, M. Cardona et al., Phys. Rev. B16, 3556 (1977).
53. I. Turyanitsa et al., Inorg. Mater., 9, 638 (1973).
54. A. Glass et al., Applied Phys. Lett. 31, 249 (1977).
55. A. Glass et al., J. Appl. Phys. 48, 5213 (1977).
56. M. Lines, Phys. Rev. B15, 388 (1977).
57. I. Turyanitsa et al., Inorg. Mater. 9, 764 (1973).
58. O. Khiminets et al., Sov. J. Glass Phys. Chem. (USA), 2, 485 (1976).
59. S. Flaschen et al., J. Appl. Phys. 31, 219 (1960).
60. D. Siapkas, Ferroelectrics, 7, 295 (1974)
61. A. Koytsoudakis, J. Louisis, A. Barzokas, D. Siapkas, Ferroelectrics, 12, 131 (1976).
62. M. Teng, M. Balkanski, M. Ziolkiewicz, Phys. St. Sol. (b), 62, 173 (1974).
63. A. Barzokas, D. Siapkas, Ferroelectrics 12, 127 (1976).
64. C. Paraskevopoulos, D. Siapkas, Ferroelectrics 23, 605 (1980).
65. G. Voutsas and P. Rentzeperis, Zeitschrift fur Kristallographie, 152, 109 (1980).

ΠΕΡΙΛΗΨΗ

# ΜΕΛΕΤΗ ΤΩΝ ΑΜΟΡΦΩΝ ΗΜΙΑΓΩΓΩΝ ΜΕ ΦΑΣΜΑΤΟΣΚΟΠΙΑ ΥΠΕΡΥΘΡΟΥ ΚΑΙ RAMAN

Ὑπὸ

Δ. Ι. ΣΙΑΠΚΑ

*(Ἐργαστήριο Β' Ἕδρας Φυσικῆς Πανεπιστημίου Θεσσαλονίκης)*

Σήμερα ἡ φασματοσκοπία Ὑπερύθρου καὶ Raman εἶναι ὑψηλοῦ ἐπιπέδου ἐργαλεῖα γιὰ τὴν μελέτη τῶν ἀτομικῶν δονήσεων, τῶν χημικῶν δεσμῶν καὶ τὴν τοπικὴ διευθέτηση τῶν ἀτόμων κατὰ ἕνα τρόπο συμπληρωματικὸ τῶν μεθόδων περιθλάσεως ἀκτίνων X, ἠλεκτρονίων καὶ νετρονίων. Ἡ ἐργασία παρέχει μία φυσικὴ εἰκόνα τῆς ἄμορφης κατάστασης, τῆς καταστροφῆς τῶν κανόνων ἐπιλογῆς τῆς κρυσταλλικῆς κατάστασης καὶ τῆς ἐμφάνισης νέων δονητικῶν φασμάτων IR καὶ Raman λόγω τῆς ἀταξίας. Ἐπιπλέον παρουσιάζονται οἱ φυσικὲς ἀρχὲς πού διέπουν τὴν λήψη, τὴν ἀνάλυση καὶ ἑρμηνεία τῶν φασμάτων IR καὶ Raman. Οἱ μέθοδοι ἐφαρμόζονται παραδειγματικὰ στοὺς πρότυπους τετραεδρικοὺς Ge, Si, GaAs, καὶ τῆς ὁμάδας χαλκογενιδίων ἀμόρφων ἡμιαγωγῶν, στοιχειακῶν καὶ ἑνώσεων καθὼς καὶ στὰ δυαδικὰ κράμματα $As_{1-x}Se_x$ καὶ Si-H. Ἀκόμη περιγράφονται τὰ φάσματα δονήσεων τῆς σιδηροηλεκτρικῆς ἡμιαγωγικῆς ἕνωσης SbSBr καὶ τοῦ στερεοῦ διαλύματος $[AsSI]_{1-x}$ - $[SbSI]_x$ κατὰ τὴν μετατροπὴ τῆς κρυσταλλικῆς κατάστασης σὲ ἄμορφη.